

**AN EFFICIENT BAYESIAN APPROACH TO HISTORY
MATCHING AND UNCERTAINTY ASSESSMENT**

A Thesis

by

CHENGWU YUAN

Submitted to the Office of Graduate Studies of
Texas A&M University
in partial fulfillment of the requirements for the degree of

MASTER OF SCIENCE

December 2005

Major Subject: Petroleum Engineering

**AN EFFICIENT BAYESIAN APPROACH TO HISTORY
MATCHING AND UNCERTAINTY ASSESSMENT**

A Thesis

by

CHENGWU YUAN

Submitted to Office of Graduate Studies of
Texas A&M University
in partial fulfillment of the requirements for the degree of

MASTER OF SCIENCE

Approved by:

Chair of Committee,	Akhil Datta-Gupta
Committee Members,	J. Bryan Maggard Yalchin Efendiev
Head of Department,	Stephen A. Holditch

December 2005

Major Subject: Petroleum Engineering

ABSTRACT

An Efficient Bayesian Approach to History Matching and Uncertainty Assessment.

(December 2005)

Chengwu Yuan, B.S., China University of Petroleum, China;

M.S., University of Petroleum, Beijing, China

Chair of Advisory Committee: Dr. Akhil Datta-Gupta

Conditioning reservoir models to production data and assessment of uncertainty can be done by Bayesian theorem. This inverse problem can be computationally intensive, generally requiring orders of magnitude more computation time compared to the forward flow simulation. This makes it not practical to assess the uncertainty by multiple realizations of history matching for field applications.

We propose a robust adaptation of the Bayesian formulation, which overcomes the current limitations and is suitable for large-scale applications. It is based on a generalized travel time inversion and utilizes a streamline-based analytic approach to compute the sensitivity of the travel time with respect to reservoir parameters. Streamlines are computed from the velocity field that is available from finite-difference simulators. We use an iterative minimization algorithm based on efficient SVD (singular value decomposition) and a numerical ‘stencil’ for calculation of the square root of the inverse of the prior covariance matrix. This approach is computationally efficient. And the linear scaling property of CPU time with increasing model size makes it suitable for large-scale applications. Then it is feasible to assess uncertainty by sampling from the posterior probability distribution using Randomized Maximum Likelihood method, an approximate Markov Chain Monte Carlo algorithms.

We apply this approach in a field case from the Goldsmith San Andres Unit (GSAU) in West Texas. In the application, we show the effect of prior modeling on posterior uncertainty by comparing the results from prior modeling by Cloud Transform and by

Collocated Sequential Gaussian Simulation. Exhausting prior information will reduce the prior uncertainty and posterior uncertainty after dynamic data integration and thus improve the accuracy of prediction of future performance.

DEDICATION

To beloved God, to my wife, to my parents, to my sisters, to all who had been or are working with me in this research group.

ACKNOWLEDGMENTS

I would like to express my appreciation to God, for giving me opportunity to work in this splendid group, and giving me persistence, patience and help in doing this work.

I would like to express my great and sincere gratitude to my graduate advisor, Dr. Akhil Datta-Gupta, for his financial support, academic guidance and his amazing class in streamline simulation, inverse theory and practice and in geostatistics.

I would like to thank Dr. Bryan Maggard for serving as committee member, for teaching me the advanced reservoir engineering and applied reservoir simulation, and for the accessibility for discussion.

I would like to thank Dr. Yalchin Efendiev for serving as committee member, and for teaching me the MCMC and its applications in stochastic modeling.

I want to thank my friends in the research group: Dr. Zhong He (now with Schlumberger), Dr. Ahmed Dauod (now with Schlumberger), Dr. Leonardo Vega (now with Schlumberger), Dr. Xianlin Ma, Ichiro Osako, Hao Cheng, Dayo Oyerinde, Mishal Al-Harbi, Eduardo Jimenez, Fady Chaban, Deepak Devegowda for the discussions, sharing of knowledge and for making my first two years in the U.S.A. unforgettable.

I would like to acknowledge financial support from the *Joint Industry Project* members.

Many thanks to Sarah Buckingham, who helps me in dealing with admission, reinstatement, degree plans and routines from the Office of Graduate Studies. I kept bothering her with my troubles. Thanks to Dr. Hoditch for the enlightening seminars and relevant suggestions. Thanks to Eleanor and Sarah for making this seminar smooth.

Thanks to Shanqing Luo, who leads me into the right way to the belief of God.

My sincere gratitude goes to my beloved wife, for her continuous support and patience.

TABLE OF CONTENTS

	Page
ABSTRACT	iii
DEDICATION	v
ACKNOWLEDGMENTS.....	vi
TABLE OF CONTENTS	vii
LIST OF FIGURES.....	ix
CHAPTER	
I INTRODUCTION	1
1.1 Introduction.....	1
1.2 Literature Review	2
1.3 Objectives.....	4
II THE EFFICIENT BAYESIAN APPROACH FOR DYNAMIC DATA INTEGRATION	5
2.1 Reformulation of Bayesian Approach.....	5
2.2 Numerically-Derived Stencil for Computing Square Root of the Inverse of the Prior Covariance Matrix.....	8
2.3 Data Misfit via Generalized Travel Time	11
2.4 Sensitivity Calculations.....	12
III UNCERTAINTY ASSESSMENT BY THE RANDOMIZED MAXIMUM LIKELIHOOD METHOD.....	14
IV APPLICATIONS IN A FIELD CASE.....	20
4.1 Introduction of Gold Smith Field.....	20
4.2 Generation of Prior Model	21
4.2.1 Generation of Prior Model by Cloud Transform.....	21
4.2.2 Generation of Prior Model by Collocated Simulation	22
4.3 Uncertainty Assessment in History Matching.....	23
4.4 Uncertainty Assessment in Prediction of Performance.....	42

CHAPTER	Page
V CONCLUSIONS AND RECOMMENDATIONS.....	52
5.1 Conclusions	52
5.2 Recommendations	53
NOMENCLATURE.....	55
REFERENCES.....	57
VITA	61

LIST OF FIGURES

FIGURE	Page
2.1 Eigenvalues for different covariance models	10
4.1 CO ₂ pilot project site, Gold Smith field	20
4.2 Extended study area, Gold Smith field.....	21
4.3a Water cut for well 1, Cloud Transform	24
4.3b Water cut for well 1, CSGS.....	25
4.4a Water cut for well 2, Cloud Transform	26
4.4b Water cut for well 2, CSGS.....	27
4.5a Water cut for well 3, Cloud Transform	28
4.5b Water cut for well 3, CSGS.....	29
4.6a Water cut for well 4, Cloud Transform	30
4.6b Water cut for well 4, CSGS.....	31
4.7a Water cut for well 5, Cloud Transform	32
4.7b Water cut for well 5, CSGS.....	33
4.8a Water cut for well 6, Cloud Transform	34
4.8b Water cut for well 6, CSGS.....	35
4.9a Water cut for well 7, Cloud Transform	36
4.9b Water cut for well 7, CSGS.....	37
4.10a Water cut for well 8, Cloud Transform	38
4.10b Water cut for well 8, CSGS.....	39
4.11a Water cut for well 9, Cloud Transform	40
4.11b Water cut for well 9, CSGS.....	41
4.12 Conditioned water cut for well 1, Cloud Transform	42
4.13 Conditioned water cut for well 2, Cloud Transform	43
4.14 Conditioned water cut for well 3, Cloud Transform	43
4.15 Conditioned water cut for well 4, Cloud Transform	44
4.16 Conditioned water cut for well 5, Cloud Transform	44

FIGURE	Page
4.17 Conditioned water cut for well 6, Cloud Transform	45
4.18 Conditioned water cut for well 7, Cloud Transform	45
4.19 Conditioned water cut for well 8, Cloud Transform	46
4.20 Conditioned water cut for well 9, Cloud Transform	46
4.21 Conditioned water cut for well 1, CSGS	47
4.22 Conditioned water cut for well 2, CSGS	47
4.23 Conditioned water cut for well 3, CSGS	48
4.24 Conditioned water cut for well 4, CSGS	48
4.25 Conditioned water cut for well 5, CSGS	49
4.26 Conditioned water cut for well 6, CSGS	49
4.27 Conditioned water cut for well 7, CSGS	50
4.28 Conditioned water cut for well 8, CSGS	50
4.29 Conditioned water cut for well 9, CSGS	51

CHAPTER I

INTRODUCTION

1. 1 Introduction

Conditioning geologic models to production data and assessment of uncertainty in models is generally done using a Bayesian formulation. The Bayesian inverse problem can be computationally intensive, generally requiring an order of magnitude more computation time compared to flow simulation itself. This makes assessment of uncertainty by examining multiple realizations practically infeasible for large-scale field applications.

Recently streamline simulators have shown great promise in this regard. Streamline models are limited in terms of their ability to account for compressible flow and complex physical mechanisms. In contrast, finite difference models have much broader applicability. Unfortunately field-scale applications of inverse modeling using finite-difference models have been mostly limited to relatively modest model sizes. This is partly because current approaches suffer from high computation costs associated with sensitivity computations and minimization algorithms.

We propose a fast and robust adaptation of the Bayesian formulation for inverse modeling that overcomes much of current limitations and is suitable for large-scale field applications. This approach is based on a generalized travel time inversion and utilizes a streamline-based analytic approach to compute the sensitivity of the travel time with respect to reservoir parameters such as porosity and permeability. The streamlines can be computed from a numerical velocity field that is readily available from finite-difference simulators. So, this approach is applicable to both finite-difference as well as streamline simulators. For solving the inverse problem, we utilize an iterative minimization algorithm based on efficient singular value decomposition and a numerical technique for

The thesis follows the style of *SPE Journal*.

the calculation of square root of the inverse of the prior covariance matrix in the Bayesian formulation. This approach is computationally efficient and more importantly the CPU time scales linearly with respect to model size. So, it is particularly suitable for large-scale field applications. It is then feasible to assess uncertainty by sampling from the posterior probability distribution using approximate Markov Chain Monte Carlo algorithms. We demonstrate the power and utility of our approach using a field example from the Goldsmith San Andres Unit (GSAU) in West Texas.

1.2 Literature Review

Conditioning geological models to production data typically require the solution of inverse problem. Such inverse problems are usually ill posed and their solutions suffer from difficulties in existence, uniqueness, and stability. To remedy these problems, a regularization term, in the form of data-independent prior information is generally added to the objective function in the inverse problem. Two different approaches to impose the regularization term have been used extensively in reservoir characterization literatures. One of these approaches is the Bayesian¹⁻⁷, and the other is the deterministic⁸⁻¹¹. Both approaches have been successfully applied for conditioning geological models to production history and comparison between the two approaches can be found in the literature^{12,13}. Unlike the deterministic approach, the Bayesian approach associates a probability distribution to the prior models and is thus considered well-suited for post-data inference and uncertainty assessment by defining a posterior distribution of models and sampling multiple realizations from this distribution. That is why we used the Bayesian approach for uncertainty assessment during this work.

Different methods are used to sample the posterior distribution for uncertainty assessment^{14,15}. This requires the solution of the Bayesian inverse problem commonly done by gradient-based algorithms of Newton-type like Gauss-Newton or modified Gauss-Newton^{16,4,5,7}. The Newton-type algorithms have quadratic rate of convergence¹⁷ in the vicinity of the solution compared to other type of search directions like quasi-

Newton which has super linear rate of convergence, the steepest descent and conjugate gradient which have linear rate of convergence.

However, the Bayesian inverse problem still suffers from three major limitations that make it impractical for field scale applications. The CPU time for Bayesian inverse problem using the conventional Gauss-Newton algorithm scales in quadratic manner with increasing the model size^{18,13}. The sensitivity calculation required by Gauss-Newton algorithm depends upon the number of model parameters¹⁹ or the number of data^{20-23, 4-6}. And high CPU time and memory required for covariance matrix calculation. Some attempts made to alleviate the third limitation associated with analytically derived stencil to approximate the inverse of the covariance matrix for large-scale field applications^{24,25}, however those are limited only for the exponential covariance models.

We propose a fast and robust adaptation of the Bayesian formulation of inverse modeling that overcomes much of current limitations and is well suited for large-scale field applications. Our approach utilizes a streamline-based analytic sensitivity computation that is computationally efficient, requires only a single flow simulation per minimization iteration and is applicable to both finite difference and streamline simulators. The production data integration relies on a generalized travel time inversion that has been shown to be extremely robust because of its quasi-linear properties²⁶. A minimization algorithm based on efficient singular value decomposition is used to solve the inverse problem. We propose a numerical ‘stencil’ for calculation of the square root of the inverse of the prior covariance matrix in the Bayesian formulation. The numerical stencil is broadly applicable to a wide class of covariance models and leads to significant savings in computation time.

Our proposed approach exhibits a linear scaling of the CPU time with respect to model size making it particularly well-suited for large-scale field applications and at the same time preserves the quadratic convergence of Gauss-Newton. It now makes it feasible to assess uncertainty by rigorously sampling from the posterior probability distribution using Markov Chain Monte Carlo algorithms. In particular, we utilize a previously proposed approximate Metropolis-Hastings sampling approach based on

randomized maximum likelihood method²⁷. The efficiency of the method lies in the fact that it ensures acceptance of all realizations that are conditioned to production data and at the same time adequately samples the uncertainty space.

We demonstrate the power and utility of our approach applying a field example from the Goldsmith San Andres Unit (GSAU) in West Texas .It includes multiple patterns consisting of 11 injectors, 31 producers and over 20 years of production history. We utilized the concept of randomized maximum likelihood to sample from the posterior for uncertainty assessment during the production history using both streamline and finite difference as the forward models. The effects of prior modeling are studied by comparing study in this application.

1.3 Objectives

The main objectives of this research are to:

- Apply an efficient Bayesian formulation that is suitable for large-scale field applications.
- Apply a novel approach, numerical stencil, to compute the square root of the inverse of the prior covariance matrix required by our Bayesian formulation, which is general to different types of covariance functions.
- Apply the generalized travel time approach with streamline-based sensitivity.
- Generate multiple prior models by sequential Gaussian simulation collocated by porosity to improve the estimation of permeability. Compare it with results obtained from cloud transform to study the effect of prior modeling in the uncertainty of matching and prediction.
- Assess the uncertainty in the matching of production history and in performance prediction for a field example to test its practical feasibility.

CHAPTER II

THE EFFICIENT BAYESIAN APPROACH FOR DYNAMIC DATA INTEGRATION

A Bayesian formulation is proposed which is applicable for both finite difference and streamline models. It has three advantages. First, use the numerically derived stencil to compute the square root of the inverse of the prior covariance and it is general for any covariance model. Second, the data misfit term, which is given as a single value, called “generalized travel time shift” at each well. Third, the analytical sensitivity based on streamline concept for finite difference models, which requires only one forward simulation run per iteration and is applicable for both streamline and finite difference models. Then, an iterative sparse matrix solver, LSQR²⁸, is used for model parameter updating. The CPU time scales linearly with increasing model size compared to the quadratic scaling^{13,18} manner in the conventional Gauss-Newton while it preserves the quadratic convergence of Gauss-Newton in the vicinity of the solution.

2.1 Reformulation of Bayesian Approach

The Bayesian approach provides a natural framework for combining prior geologic data with the dynamic production data. The objective is to derive a more refined statistical distribution for the model parameters, called the posterior distribution, which will be more tightly constrained, compared to the prior distribution. We can then explore the posterior distribution to obtain plausible models given the data. If we assume that the prior model has a multivariate Gaussian distribution with a covariance matrix C_M and the production data has Gaussian uncertainty described by the data covariance C_d , then the Bayesian approach leads to the following posterior distribution, **Eq. 2.1**.

$$P(m|d) \propto \exp \left\{ -\frac{1}{2} [d - g(m)]^T C_d^{-1} [d - g(m)] + \frac{1}{2} [m - m_p]^T C_M^{-1} [m - m_p] \right\} \dots \dots \dots (2.1)$$

Where d represents the data vector of dimension N_d , m represents the model parameter vector with dimension M and $g(m)$ defines the non-linear relationship between the model parameters and the calculated data.

We start out by re-writing the objective function in the Bayesian formulation as follows:

$$F(m) = \frac{1}{2} e^T e \dots\dots\dots (2.2)$$

Where,

$$e = \begin{bmatrix} C_d^{-1/2} (d - g(m)) \\ C_M^{-1/2} (m - m_p) \end{bmatrix} \dots\dots\dots (2.3)$$

The minimization of the objective function given in **Eq. 2.2** can be obtained by using Newton's optimization algorithm¹⁷ as follows:

$$H \delta m = -J^T e \dots\dots\dots (2.4)$$

Where the Jacobian J and the Hessian H are given by the following equations:

$$J = \nabla e \dots\dots\dots (2.5)$$

$$H \cong J^T J \dots\dots\dots (2.6)$$

The approximation for the Hessian, **Eq. 2.6**, is the same as that of the Gauss-Newton algorithm and is strictly valid near the solution (small misfit) or for quasilinear problems. We can now write **Eq. 2.4** as follows

$$J^T J \delta m = -J^T e \dots\dots\dots (2.7)$$

Notice that **Eq. 2.7** is a least-squares solution to the following system of equations

$$J\delta m = -e \dots\dots\dots (2.8)$$

$$\begin{bmatrix} C_d^{-1/2}G \\ C_M^{-1/2} \end{bmatrix} \delta m = \begin{bmatrix} C_d^{-1/2}(d - g(m)) \\ C_M^{-1/2}(m_p - m) \end{bmatrix} \dots\dots\dots (2.9a)$$

The data misfit term, $[d - g(m)]$, is given in **Eq. 2.9a** by a single value called ‘‘Generalized Travel Time Shift’’, $\Delta\tilde{t}$ at each well. This reduces the dimension of the data misfit vector to be of $n_w \times 1$, the data covariance matrix, C_D , to be of $n_w \times n_w$ and the sensitivity matrix, G , to be of $n_w \times M$. Where, n_w is the number of wells and M is the number of model parameters. The detail about the formulation of the generalized travel time shift will be discussed later in the chapter. So, **Eq. 2.9a** becomes:

$$\begin{bmatrix} C_d^{-1/2}G \\ C_M^{-1/2} \end{bmatrix} \delta m = \begin{bmatrix} C_d^{-1/2} \Delta\tilde{t} \\ C_M^{-1/2}(m_p - m) \end{bmatrix} \dots\dots\dots (2.9b)$$

Eq. 2.9b represents a system of linear equations and we use an iterative sparse matrix solver, LSQR²⁸ for solving this system. LSQR is well suited for highly ill conditioned systems and is widely used for large-scale tomography problem in seismology²⁹. However, difficulties arise in the computation of the square root of the matrix inverse in **Eq. 2.9b**. In practice, the data covariance matrix is assumed to be diagonal and is thus easy to manipulate. However, the covariance matrix for the model parameters can be full and in general, the calculation of $C_M^{-1/2}$ will be computationally prohibitive for large-scale inverse problems. Previous efforts to compute $C_M^{-1/2}$ analytically have been limited to exponential covariance model¹³. We propose an approach to approximate the square

root of the inverse of the covariance using a numerical stencil, which is general for any covariance model.

2.2 Numerically-Derived Stencil for Computing Square Root of the Inverse of the Prior Covariance Matrix

The exact analytical calculation of the square root of the inverse of the covariance can be done using the concept of matrix diagonalization³⁰. Since the covariance matrix is a symmetric matrix. The inverse of the square root can be calculated exactly using the following equation:

$$C_M^{-1/2} = U^T \Lambda^{-1/2} U \quad (2.10)$$

Where U is the matrix, whose columns are the eigenvectors of C_M , Λ is the diagonal matrix whose diagonal elements are the eigenvalues of the covariance matrix C_M . This computation is very difficult to handle especially for large field scale cases where the covariance matrix is large.

The alternative is to approximate the square root of the inverse of the covariance by obtaining analytically its stencil from the covariance kernel¹³. However, the analytical stencil suffers from two major limitations; it is applicable only for exponential covariance and the ratio of the grid size to the range in the three directions are equal.

We proposed a method that overcomes these limitations which is based on two basic principles; First, the covariance matrix and the square root of its inverse can be constructed using their respective kernels, Second, the two kernels remain unchanged regardless of the size of the matrix.

The following are the steps used to approximate the square root of the inverse of the covariance matrix using a numerically derived stencil.

In step 1, we set up a size of the stencil, we found that 5x5x5 stencil provided a good compromise between efficiency and accuracy, so we used 5x5x5 stencil to approximate the square root of the inverse of the covariance.

In step 2, we use the matrix diagonalization given in **Eq. 2.10** to get the square root of the inverse of the covariance for 5x5x5 grid block (125x125 covariance matrix) by knowing the kernel of the covariance. This is equivalent to getting the kernel of the square root of the inverse of any covariance function in a discretized or numerical form other than obtaining the kernel analytically, which is too complicated especially for the Gaussian and spherical covariance models.

In step 3, we set up the 5x5x5 stencil. This stencil has only 27 distinct elements due to symmetry. We use any column or any row of the covariance matrix calculated from the second step to get the value of stencils. Finally, we use the stencil from second step to construct the exact matrix of the model size under study.

This technique provides a good approximation for the exponential, the spherical and the Gaussian models. And the constraint imposed by the analytical technique—that the ratio of the grid sizes to the ranges in the three directions of anisotropy must be constant—has been removed.

To justify this approach, the eigenvalues of covariance matrix from different models are calculated in a synthetic case as shown in **Table 2.1**. From **Fig. 2.1** (a), (b) and (c), we can see that, with range increase, the eigenvalues of covariance matrix decrease steeply for these three models. If we set a small cut off, only a small part of the grids in the range contribute much to the estimate. So, when the range is high, the 5x5x5 stencil will catch the high values above a small cut off. When the range is low, the 5x5x5 stencil is enough to cover most parts or all of the range. That is why the numerical stencil gives good approximation.

Table 2.1 – Data used to generate covariance matrix for the illustrative example							
Model	σ^2	Δx	Δy	Δz	Nx	Ny	Nz
Exp	1.00	0.04	0.15	0.4	12	7	13
Sph	1.00	0.04	0.15	0.4	12	7	13
Gauss	1.00	0.43	0.41	0.5	12	7	13

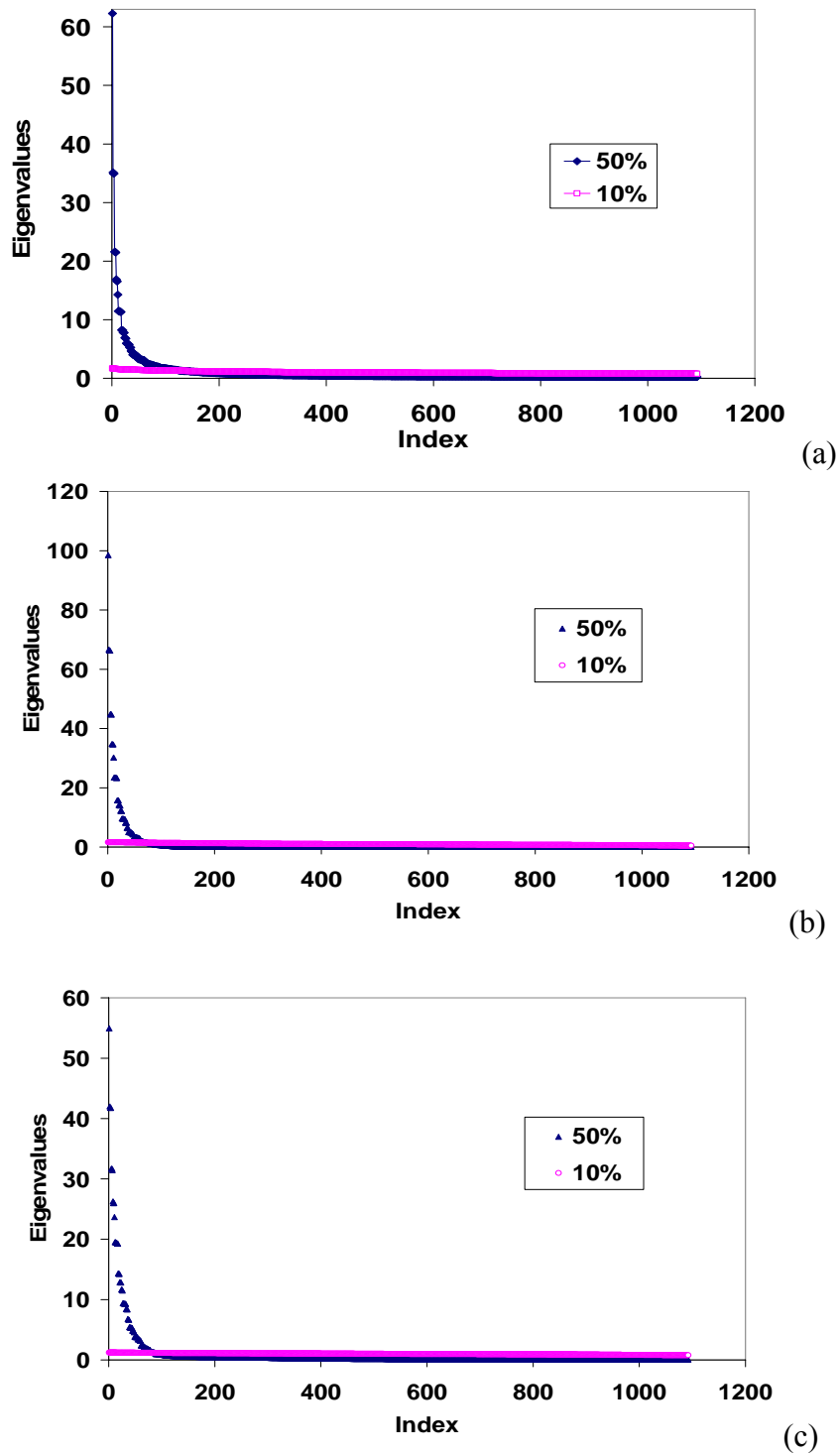


Fig. 2.1 – Eigenvalues for different covariance models. (a) Exponential, (b) Gaussian, (c) Spherical

2.3 Data Misfit via Generalized Travel Time

Production data misfit is most commonly represented as follows

$$J_p = \sum_{j=1}^{n_w} \sum_{i=1}^{n_{dj}} w_{ij} (y_j^{cal}(t_i) - y_j^{obs}(t_i))^2 \dots\dots\dots (2.11)$$

For $i = 1, \dots, n_{dj}$, $j = 1, \dots, n_w$.

In the above equation, $y_j(t_i)$ denotes the production data for well j at time t_i , n_w and n_{dj} stand for the number of production wells and the number of observed data at each well, respectively and w_{ij} represent the data weights. Instead, we define a ‘generalized travel-time’ whereby we seek an optimal time-shift at each well to minimize the production data misfit at the well. Taking well j as an example, the optimal shift will be given by the t_j that minimizes the misfit function,

$$J_p = \sum_{i=1}^{N_{dj}} [y_j^{obs}(t_i + \Delta t_j) - y_j^{cal}(t_i)]^2 = f(\Delta t_j) \dots\dots\dots (2.12)$$

Or, alternatively maximizes the coefficient of determination given by the following

$$R^2(\Delta t_j) = 1 - \frac{\sum [y_j^{obs}(t_i + \Delta t_j) - y_j^{cal}(t_i)]^2}{\sum [y_j^{obs}(t_i) - \overline{y_j^{obs}}]^2} \dots\dots\dots (2.13)$$

Thus, we define the generalized travel-time as the ‘optimal’ time-shift $\Delta \tilde{t}_j$ that maximizes $R^2(\Delta t_j)$ or minimizes J_p . It is important to point out that the computation of the optimal time-shift does not require any additional flow simulations. It is carried out as a post-processing at each well after the calculated production response is derived using a flow simulation. The overall production data misfit can now be expressed in terms of a generalized travel-time misfit at all wells as follows

$$E = \sum_{j=1}^{N_w} (\Delta \tilde{t}_j)^2 \dots \dots \dots (2.14)$$

2.4 Sensitivity Calculations

One important aspect of this formulation is computation of the sensitivity matrix G as in **Eq. 2.9a**, which relates the production response to model parameters. Although several methods are available for computing sensitivities, for example, perturbation method, or ad joint state method, which are limited by their computational costs and complex implementations. Streamline-based analytic sensitivity computation approach is extremely efficient and requires only a single simulation run. We use a streamline-based analytic approach for this purpose. The streamline-based sensitivity computation can be used for both streamline and finite-difference simulators¹¹. For finite difference simulators, we first trace the streamline trajectories from the fluid fluxes obtained from the simulator. We can then compute the time of flight and parameter sensitivities as discussed in several of our previous publications^{10,11,26}.

In generalized travel time inversion (GTTI), every data point in the fractional-flow curve has the same shift time, that is, $\Delta \tilde{t}^1 = \Delta \tilde{t}^2 = \dots = \Delta \tilde{t}^L = \Delta \tilde{t}$. So we can sum up and average the travel time sensitivities of all data points to obtain a rather simple expression for the sensitivity of the generalized travel time with respect to reservoir parameters m at well j as follows¹⁰

$$\frac{\partial \Delta \tilde{t}_j}{\partial m} = \frac{\sum_{i=1}^{N_{dj}} (\partial t_{i,j} / \partial m)}{N_{dj}} \dots \dots \dots (2.15)$$

It now reduces to the sensitivity of the arrival times at the producing well j , $\partial t_{i,j} / \partial m$. These sensitivities can be easily obtained in terms of the sensitivities of the streamline time of flight¹⁰,

$$\frac{\partial t}{\partial m} = \frac{\frac{\partial \tau}{\partial m}}{\frac{\partial f_w}{\partial S_w}} \dots\dots\dots(2.16)$$

In the above expression, the fractional flow derivatives are computed at the saturation of the outlet node of the streamline. The time of flight sensitivities can be obtained analytically in terms of simple integrals along streamline. For example, the time of flight sensitivity with respect to permeability will be given by⁷

$$\frac{\partial \tau}{\partial k(\mathbf{x})} = \int_{\Sigma} \frac{\partial s(\mathbf{x})}{\partial k(\mathbf{x})} dx = - \int_{\Sigma} \frac{s(\mathbf{x})}{k(\mathbf{x})} dx \dots\dots\dots(2.17)$$

Where, the integrals are evaluated along the streamline trajectory, and the ‘slowness’, which is the reciprocal of interstitial velocity, is given by

$$s(\mathbf{x}) = \frac{\phi(\mathbf{x})}{\lambda_r k(\mathbf{x}) |\nabla P(\mathbf{x})|} \dots\dots\dots(2.18)$$

Note that the quantities in the sensitivity expressions are either contained in the initial reservoir model or are available after the forward simulation run.

CHAPTER III

UNCERTAINTY ASSESSMENT BY THE RANDOMIZED MAXIMUM LIKELIHOOD METHOD

Uncertainty is usually evaluated from the simulated performance of a small number of reservoir models. Unfortunately, most of the methods for creating reservoir models conditional to production data are known to generate a distribution of realizations that is only approximately correct. The correctness of the approximations is unknown, although several investigations of the approximate algorithms have suggested that the distribution of realizations could be seriously deceptive.

Liu *et al.*¹⁴ evaluate the ability of the various sampling methods to correctly assess the uncertainty in reservoir predictions by comparing the distribution of realizations with a standard distribution from a Markov Chain Monte Carlo method. This study compares the ensemble of realizations from five sampling algorithms for a synthetic, one-dimensional, single-phase flow problem in order to establish the best algorithm under controlled conditions. The small test problem was chosen in order that a sufficiently large number of realizations could be generated from each method to ensure the statistical validity of the comparisons.

The methods evaluated belong to two types: those that are known to sample correctly, and those that are only approximately correct. In the first category, they consider the Rejection algorithm and a Markov Chain Monte Carlo algorithm. The three approximate methods include Linearization about the Maximum a Posteriori, Randomized Maximum Likelihood, and Pilot Point methods.

From this study, it appears that, of the methods considered, generating realizations using the Randomized Maximum Likelihood (RML) method is the only practical alternative that provides acceptable assessment of uncertainty.

Kitanidis³⁰ and Oliver, He, and Reynolds²⁷ proposed that unconditional realizations from a Gaussian random field could be used to generate realizations conditional to nonlinear data by a process of minimization. If the prior covariance of the reservoir

model parameters and the variance of the observed data are known, samples can be generated in the following way:

Step1: Generate an unconditional realization of the reservoir model parameters,

$$m_u \leftarrow N[m_{pr}, C_M] \dots\dots\dots (3.1)$$

Step2: Generate a realization of the data,

$$d_u \leftarrow N[d_{obs}, C_D] \dots\dots\dots (3.2)$$

Step3: Compute the set of model variables, m , that minimizes the function:

$$S(m) = \frac{1}{2}(m - m_u)^T C_M^{-1}(m - m_u) + \frac{1}{2}[g(m) - d_u]^T C_D^{-1}[g(m) - d_u] \dots\dots\dots (3.3)$$

The minimization step is similar to the computation of the maximum a posteriori estimate, with the difference that the regularization is with respect to unconditional realizations of the model and the data instead of the prior model and the observed data.

Oliver, *et al.*²⁷ originally suggested that this method be used to generate trial states for a Markov Chain Monte Carlo algorithm but, because the acceptance criterion was difficult to evaluate and the acceptance rate was very high (approximately 95% for a small highly nonlinear problem), they suggested that the acceptance test be ignored and all trials accepted. Because the method seeks to minimize the data mismatch and the distance from the unconditional realization, the realizations almost surely honor the data and appear to be from the correct distribution.

The procedure proposed by Oliver *et al.*²⁷ to ensure that the realizations that are generated are distributed correctly is to use the calibrated realizations as trial states in a Markov Chain Monte Carlo (MCMC) method. However, in order to be able to use the MCMC method, we need to be able to calculate the probability of proposing the

calibrated model. The state m_{cal} that is proposed is the result of calibrating the unconditioned realization to the unconditioned data (observed data plus noise) using the **Eq. 3.3**. The joint probability density, $f(m_{us}, d_{us})$ of proposing (m_{us}, d_{us}) , is easily calculated since m_{us} and d_{us} are independent random variables. Hence, for this problem,

$$f(m_{us}, d_{us}) \propto \exp\left\{-\frac{1}{2}(m_{us} - \mu)^T C_M^{-1} \frac{1}{2}(m_{us} - \mu)^T - \frac{1}{2}[d_{us} - d_{obs}]^T C_D^{-1} [d_{us} - d_{obs}]\right\} \dots (3.4)$$

The joint probability density, $h(m_{cal}, d_{us})$, of proposing (m_{cal}, d_{us}) can, theoretically be calculated if the functional relationship between (m_{us}, d_{us}) and (m_{cal}, d_{us}) is known.

In their procedure, they calculate m_{cal} using a Gauss-Newton method to find the minimum of **Eq. 3.3**, given m_{us} and d_{us} . Reversing the procedure, m_{us} can be solved for as a function of m_{cal} and d_{us} . Excluding the regions of the (m_{cal}, d_{us}) space that are inaccessible to the calibration routine, we obtain a unique one-to-one, invertible, relationship between (m_{us}, d_{us}) and (m_{cal}, d_{us}) . The joint probability of proposing (m_{cal}, d_{us}) can then be calculated as follows³¹

$$h(m_{cal}, d_{us}) = f(m_{us}, d_{us}) \cdot J \dots (3.5)$$

where, J is the Jacobian of the transformation.

$$J = \left| \frac{\partial m_{us}}{\partial m_{cal}} \right| \dots (3.6)$$

The probability of proposing m_{cal} is found by integrating $h(m_{cal}, d_{us})$ over the data space.

$$q(m_{cal}) = \int_D h(m_{cal}, d_{us}) dd_{us} \dots\dots\dots (3.7)$$

For most practical problems, evaluation of the integral in Eq. 3.7 is too difficult to attempt. The authors then present a one-dimensional example for which the calculation can be attempted, and then show an approximation that seems to work well under a fairly broad range of conditions.

If the probability of proposing a transition to state m_j is independent of the current state, Hasting's rule for the acceptance of a proposed transition from state m_i to state m_j can be written as

$$\alpha_{i,j} = \min\left(1, \frac{\pi_j q_i}{\pi_i q_j}\right) \dots\dots\dots (3.8)$$

q_j is the probability of proposing the conditioned model and depends only on the proposed state. The probability density of the conditioned model, π_j is

$$\pi_j \propto \exp\left\{-\frac{1}{2}(m_j - \mu)^T C_M^{-1}(m_j - \mu) - \frac{1}{2}[g(m_j) - d_{obs}]^T C_D^{-1}[g(m_j) - d_{obs}]\right\} \dots\dots\dots (3.9)$$

Note that the probability is not based on the quality of the match obtained in the minimization, but on the quality of the match to the prior model and the observed data.

Oliver, *et al.*²⁷ demonstrated that, for linear problems, all calibrated reservoir models would be accepted by a Metropolis-Hastings algorithm. For small nonlinear problems, they observed that accepting all calibrated models resulted in a reasonable approximation to the correct distribution. Then, they bring up the question of whether there is any reason to believe that it might be a valid method of sampling for large multivariate problems.

They start by considering the probability density for proposing calibrated models. First, new states m_{us} and d_{us} are proposed from the Gaussian prior distribution,

$$f(m_{us}, d_{us}) \propto \exp\left\{-\frac{1}{2}(m_{us} - \mu)^T C_M^{-1} \frac{1}{2}(m_{us} - \mu)^T - \frac{1}{2}[d_{us} - d_{obs}]^T C_D^{-1} [d_{us} - d_{obs}]\right\} \dots (3.10)$$

A calibrated model, m_{cal} , is got from m_{us} and d_{us} by minimizing with respect to m .

$$O(m) = \frac{1}{2}(m - m_{us})^T C_M^{-1} (m - m_{us}) + \frac{1}{2}[g(m) - d_{us}]^T C_D^{-1} [g(m) - d_{us}] \dots (3.11)$$

If the minimization is “good,” $O(m_{cal})$ will be relatively small. The m_{cal} and $g(m_{cal})$ will be close to m_{us} and d_{us} , respectively. In this case, the meaning of “close” is with respect to the weighted L_2 norm. Let $\varepsilon = m_{cal} - m_{us}$ and $\eta = g(m_{cal}) - d_{us}$. In terms of ε and η the distribution from which states are proposed can be written as

$$f(d_{us}, m_{us}) \propto \exp\left\{-\frac{1}{2}(m_{cal} - \varepsilon - \mu)^T C_M^{-1} (m_{cal} - \varepsilon - \mu) - \frac{1}{2}[g(m_{cal}) - \eta - d_{obs}]^T C_D^{-1} [g(m_{cal}) - \eta - d_{obs}]\right\} \dots (3.12)$$

where, m_{cal} , ε and η must be thought of as functions of m_{us} and d_{us} . Reorganization of the terms results in an equivalent expression in which the first two terms of the argument of the exponential are independent of ε and η

$$f(d_{us}, m_{us}) \propto \exp\left\{-\frac{1}{2}(m_{cal} - \mu)^T C_M^{-1} (m_{cal} - \mu) - \frac{1}{2}[g(m_{cal}) - d_{obs}]^T C_D^{-1} [g(m_{cal}) - d_{obs}]\right\}$$

$$\begin{aligned}
& + \varepsilon^T C_M^{-1} (m_{cal} - \mu) - \frac{1}{2} \varepsilon^T C_M^{-1} \varepsilon \\
& + \eta^T C_D^{-1} [g(m_{cal}) - d_{obs}] - \frac{1}{2} \eta^T C_D^{-1} \eta \} \dots\dots\dots (3.13)
\end{aligned}$$

The probability density of proposing a state, m_{cal} , can be obtained by multiplying **Eq. 3.13** by the Jacobian of the transformation between m_{us} and m_{cal} , then integrating over the data space. We formally write this as

$$\begin{aligned}
q(m_{cal}) \propto \exp \left\{ -\frac{1}{2} (m_{cal} - \mu)^T C_M^{-1} (m_{cal} - \mu) - \frac{1}{2} [g(m_{cal}) - d_{obs}]^T C_D^{-1} [g(m_{cal}) - d_{obs}] \right\} \\
\int_{D_{us}} \exp \left\{ \varepsilon^T C_M^{-1} (m_{cal} - \mu) - \frac{1}{2} \varepsilon^T C_M^{-1} \varepsilon + \eta^T C_D^{-1} [g(m_{cal}) - d_{obs}] - \frac{1}{2} \eta^T C_D^{-1} \eta \right\} |J| dd_{us} \dots\dots (3.14)
\end{aligned}$$

Now we must treat J , ε and η as functions of m_{cal} and d_{us} . The term outside the integral is the posterior probability density for the model. The Metropolis-Hastings acceptance criterion depends only on the ratio $\pi_j q_i / \pi_i q_j$. If this ratio is equal to one then the proposed transition to state j should be accepted. Direct computation of the ratio gives

$$\frac{\pi_j q_i}{\pi_i q_j} = \frac{\int_{D_{us}} \exp \left\{ \varepsilon_i^T C_M^{-1} (m_i - \mu) - \frac{1}{2} \varepsilon_i^T C_M^{-1} \varepsilon_i + \eta_i^T C_D^{-1} [g(m_i) - d_{obs}] - \frac{1}{2} \eta_i^T C_D^{-1} \eta_i \right\} |J_i| dd_{us}}{\int_{D_{us}} \exp \left\{ \varepsilon_j^T C_M^{-1} (m_j - \mu) - \frac{1}{2} \varepsilon_j^T C_M^{-1} \varepsilon_j + \eta_j^T C_D^{-1} [g(m_j) - d_{obs}] - \frac{1}{2} \eta_j^T C_D^{-1} \eta_j \right\} |J_j| dd_{us}} \dots\dots (3.15)$$

It seems unlikely that useful bounds can be placed on this ratio for general nonlinear functions g but, because ε and η (which are small) occur in every term within the integral in **Eq. 3.15**, the authors claim that the ratio is of the order of one in the regions of interest.

CHAPTER IV

APPLICATION IN A FIELD CASE

In this chapter, the efficient Bayesian formulation Bayesian formulation along with the RML method is applied to one field scale case, the Gold Smith Field.

4.1 Introduction of Gold Smith Field

We have applied the RML method along with the efficient Bayesian formulation to a CO₂ pilot project area in the Gold Smith San Andres Unit (GSAU), a dolomite formation in west Texas. The pilot area consists of nine inverted 5-spot patterns covering around 320 acres with average thickness of 100 ft and has over 50 years of production history prior to CO₂ project initiation in Dec 1996. The water flooding production history prior to the CO₂ injection is integrated. **Fig. 4.1** shows the CO₂ pilot project site in the GSAU.

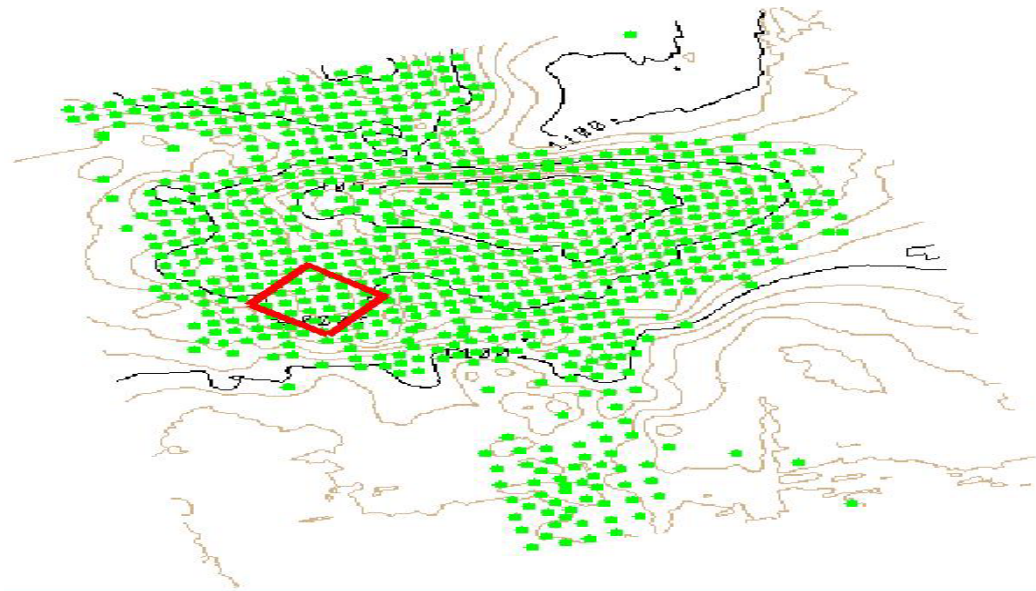


Fig. 4.1 – CO₂ pilot project site, Gold Smith field

The extended study area is shown in **Fig. 4.2** with 11 injectors and 31 producers.

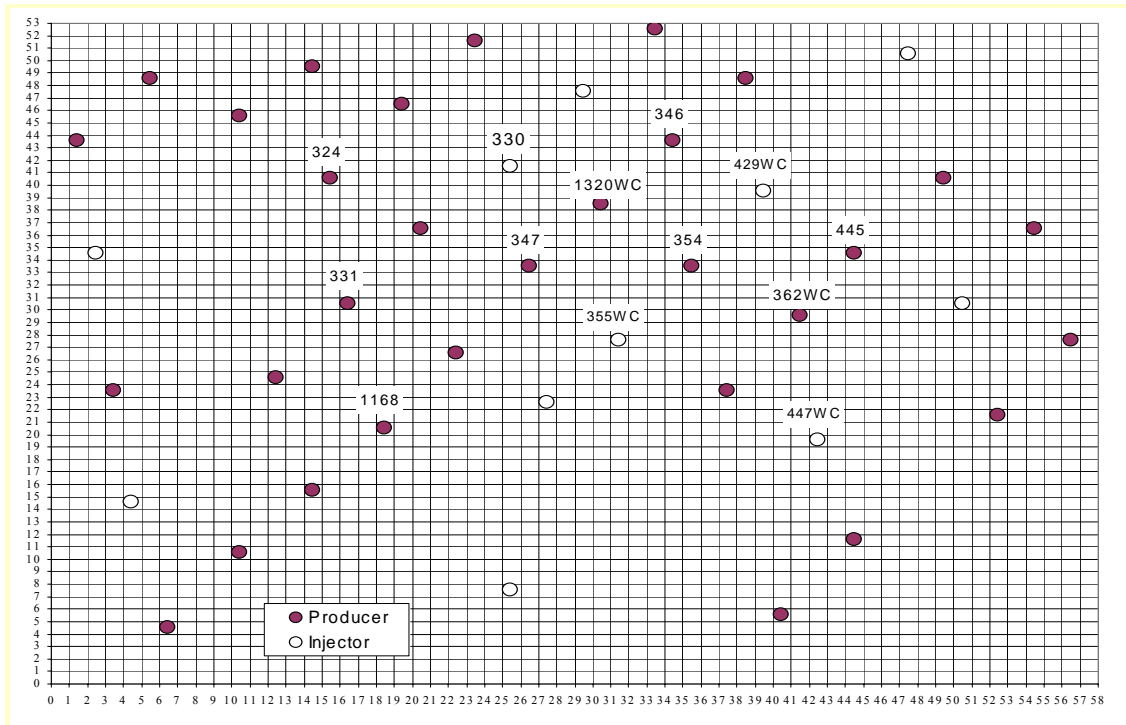


Fig. 4.2 – Extended study area, Gold Smith field

The porosity field was generated from log data using Sequential Gaussian Simulation. It was not allowed to change during the integration.

4.2 Generation of Prior Permeability Model

The stochastic modeling of prior permeability is the start point of assessment of uncertainty. In this application, cloud transform³² and Collocated Sequential Gaussian Simulation are used to generate the prior permeability field. The results will show how important it is to exhaust the available prior static information.

4.2.1 Generation of Prior Model by Cloud Transform

A cloud transform use the scatter or uncertainty in the relationship between porosity and permeability to generate permeability fields. It involves the following steps:

Step 1: Construct a probability field. This basically consists of assigning a CDF value to each grid block. This is attained using a geostatistic model such as a Sequential Gaussian Simulation or a moving average technique.

Step 2: For each grid block,

- a. Pick the value of porosity.
- b. Pick the corresponding values of permeability from the porosity-permeability relationship, and generate a permeability distribution.
- c. Sample the permeability distribution using the value of CDF corresponding to that particular grid block.

Step 3: Use the permeability obtained in **2c** as the unconditioned permeability of that particular grid block.

Step 4: Repeat steps **2** and **3** for all other grid blocks.

Forward runs were made using each of the prior permeability fields by **Eclipse 2004a**. Five unconditioned realizations of the water cut were generated by adding a randomly generated Gaussian error with a standard deviation of 0.03 to the observed water cut. The unconditioned water cuts are shown in **Figs. 4.3a (a)** to **4.11a (a)**.

4.2.2 Generation of Prior Model by Collocated SGS

Cokriging vs. Collocated Cokriging

This Cokriging estimation involves complicated system of equations and requires modeling variograms of permeability and porosity and cross-variogram of them.

$$K_{cok}(\mathbf{x}_0) = \sum_i \lambda_i K(\mathbf{x}_i) + \sum_j \mu_j \phi(\mathbf{x}_j) \dots\dots\dots(4.1)$$

The target variable, permeability, is sparsely sampled at well sites. While the auxiliary variable, the porosity, are available in all grids. In such case, collocated cokriging is a good approximation and simplification of strict cokriging. In its strict sense, collocated cokriging makes use of the auxiliary variable only at the current point where the target variable is to be estimated.

$$K_{cok}(\mathbf{x}_0) = \sum_i \lambda_i K(\mathbf{x}_i) + \lambda_{k,\phi} \cdot \phi(x_0) \dots\dots\dots(4.2)$$

In the multi-located form, it also makes use of the auxiliary variable at all points where the target variable is available. In this case, the collocated cokriging is used to generate the prior distribution of permeability with the aid of available porosity.

Collocated Sequential Gaussian Simulation (CSGS)

Construction of a permeability fields by CSGS involves the following steps:

Step 1: Select a random location in the grid scheme.

Step 2: Perform collocated kriging and get values of Z^* and $\text{Var}Z^*$.

Step 3: Assume Z^* and $\text{Var}Z^*$ are the mean and variance of a normal distribution, Sample from this distribution and assign a value as simulated value of this grid.

Step 4: Select another location.

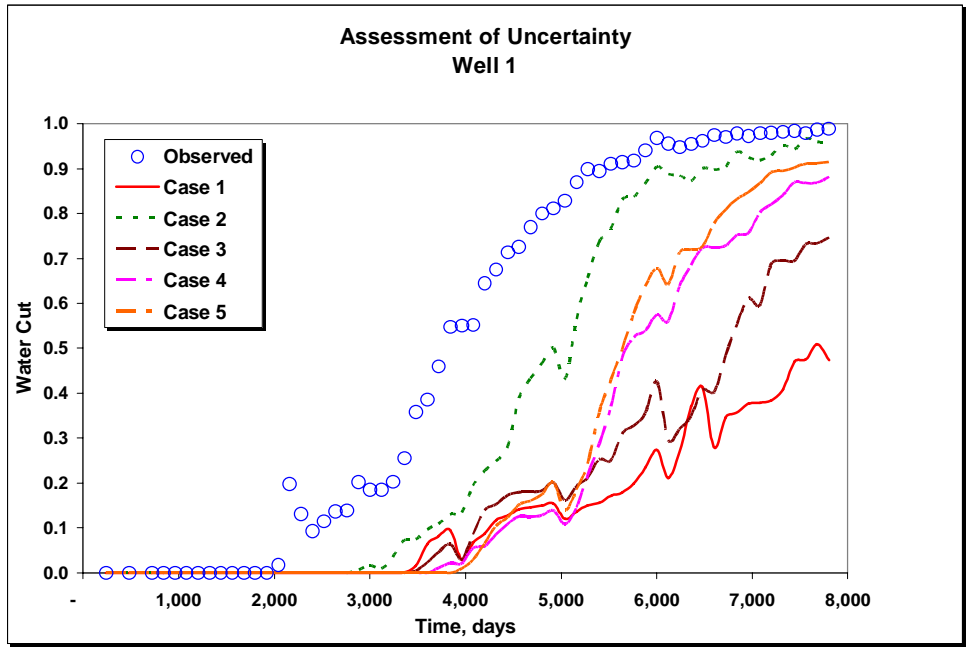
Step 5: Perform collocated kriging by latest simulated values. And get Z^* and $\text{Var}Z^*$;

Step 6: Repeat Step 3~ Step 5 until all grids are visited.

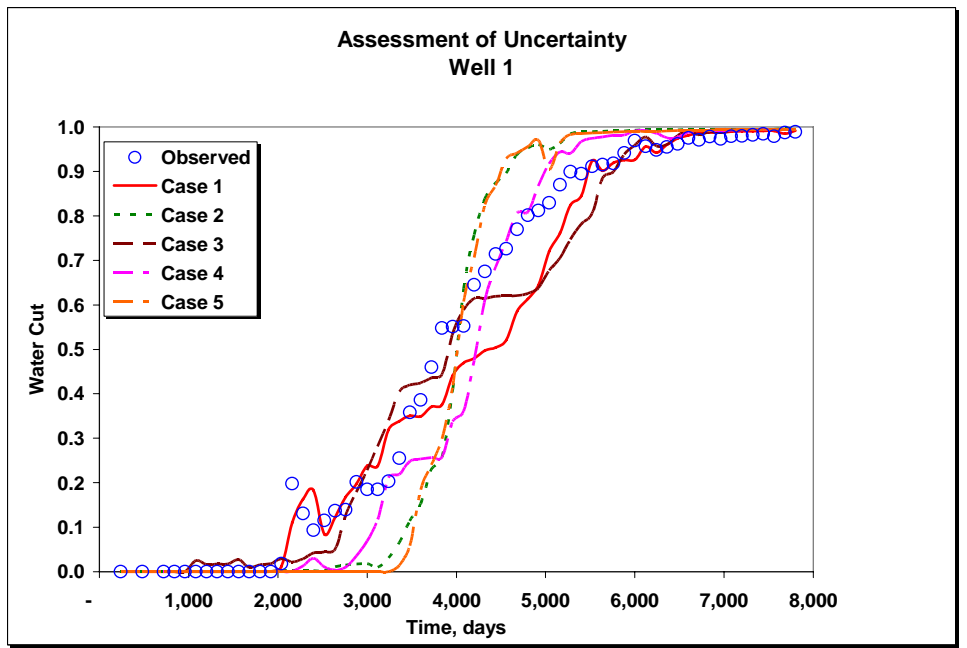
4.3 Uncertainty Assessment in History Matching

The available data are 7800-day water cut. Ten unconditioned water cut were generated by adding a randomly Gaussian error with a standard deviation of 0.03 to the observed water cut. To integrate the unconditioned permeability and water cut data, the efficient Bayesian formulation are applied. The prior model by cloud transform and collocated simulation are integrated with water cut respectively.

The results of unconditioned water cut and conditioned water cut are shown as **Figs. 4.3 (a) to 4.11 (a)** and **Figs. 4.3 (b) to 4.11 (b)**, respectively, for prior modeling by cloud transform. The results of conditioned water cut are shown as **Figs. 4.3 (a) to 4.11 (a)** and **Figs. 4.3 (b) to 4.11 (b)**, respectively, for prior modeling by collocated Gaussian sequential simulation.

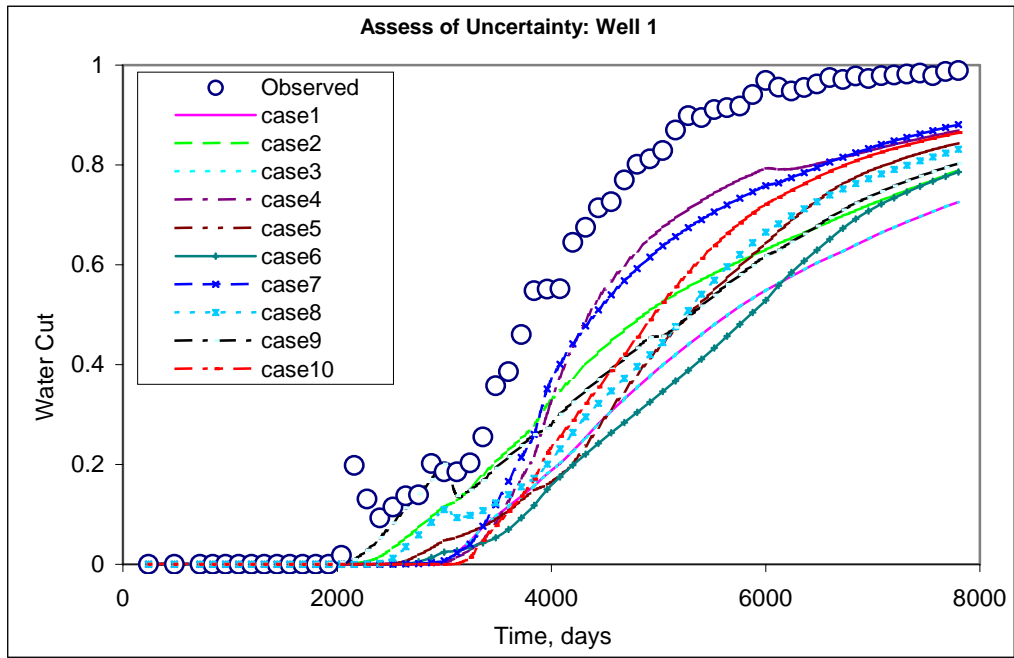


(a)

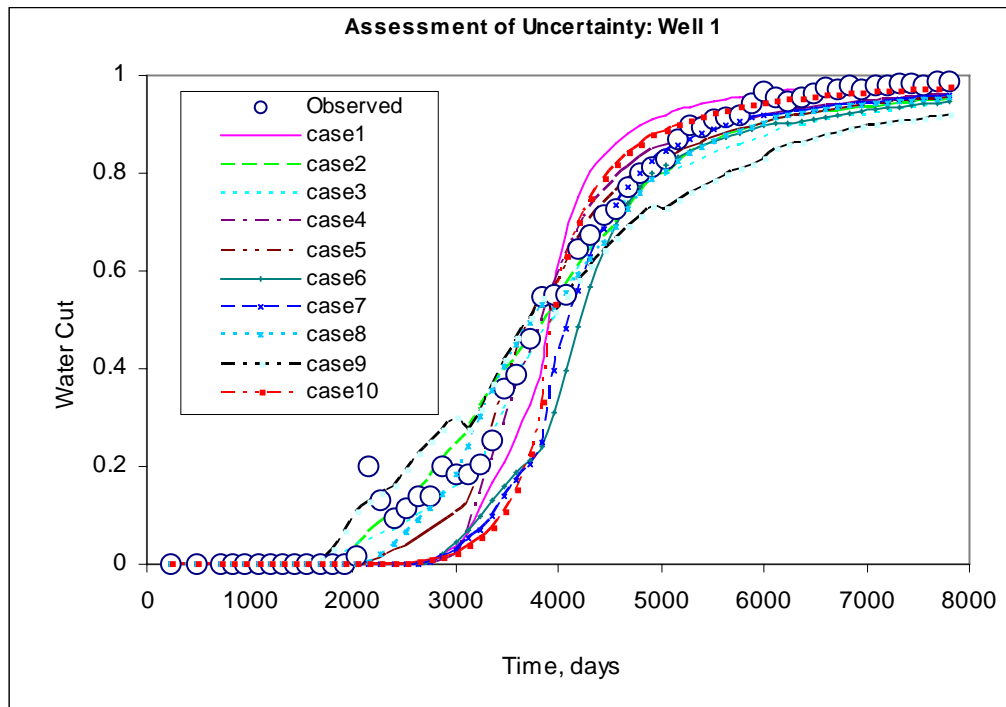


(b)

Fig. 4.3a– Water cut for well 1, Cloud Transform. (a) Unconditioned, (b) Conditioned

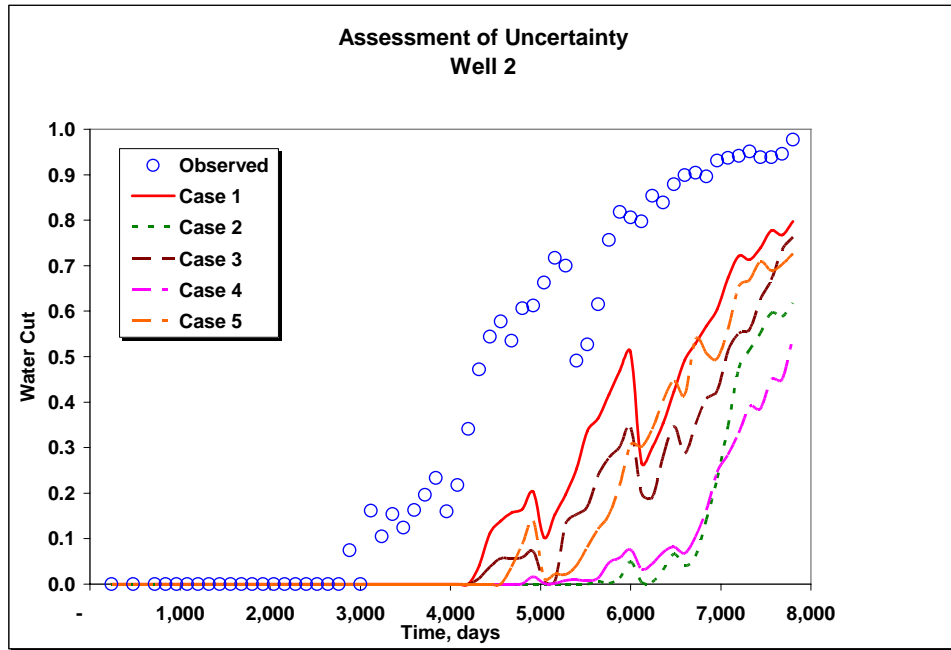


(a)

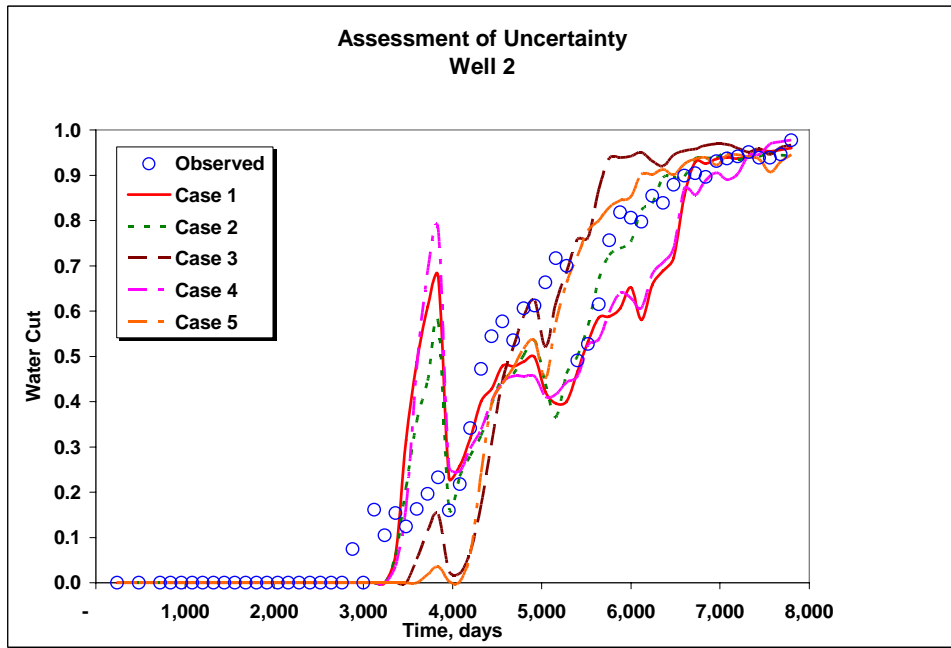


(b)

Fig. 4.3b– Water cut for well 1, CSGS. (a) Unconditioned, (b) Conditioned

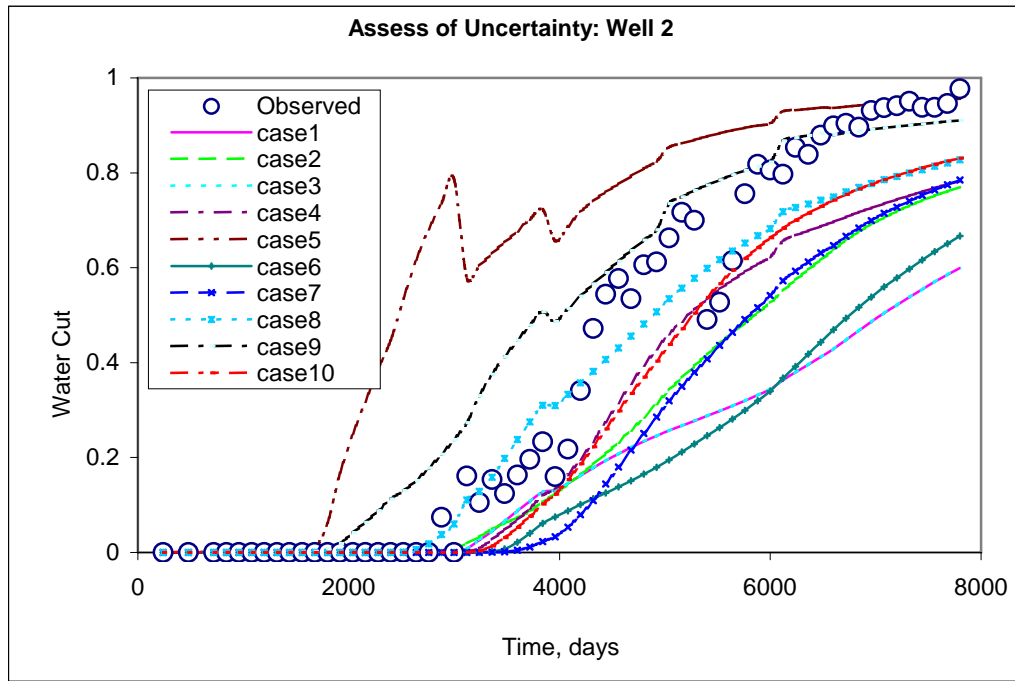


(a)

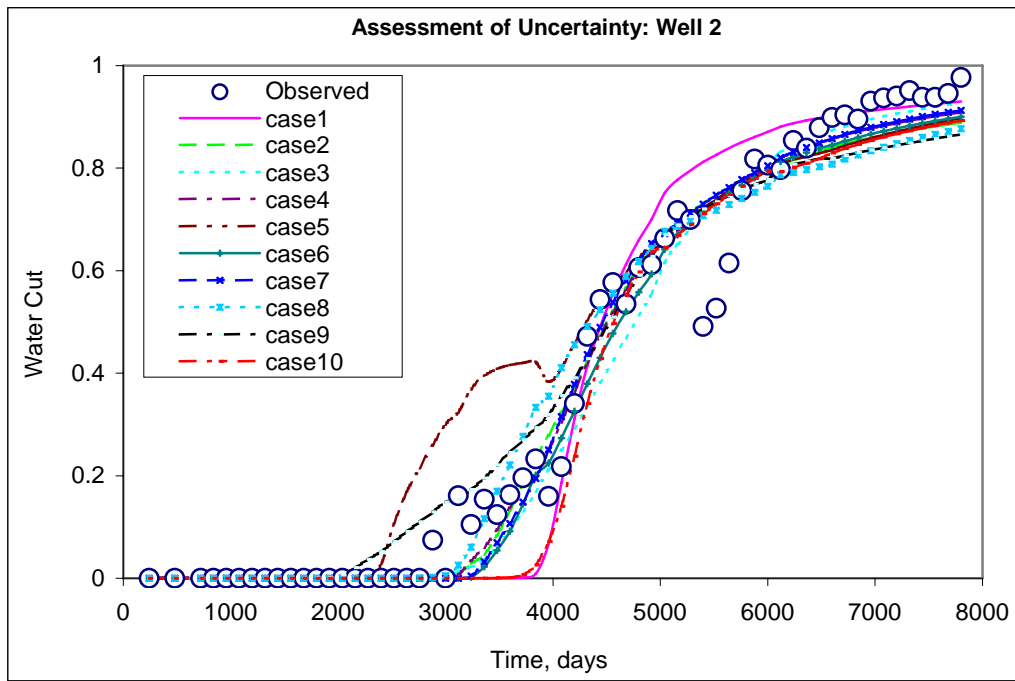


(b)

Fig. 4.4a– Water cut for well 2, Cloud Transform. (a) Unconditioned, (b) Conditioned

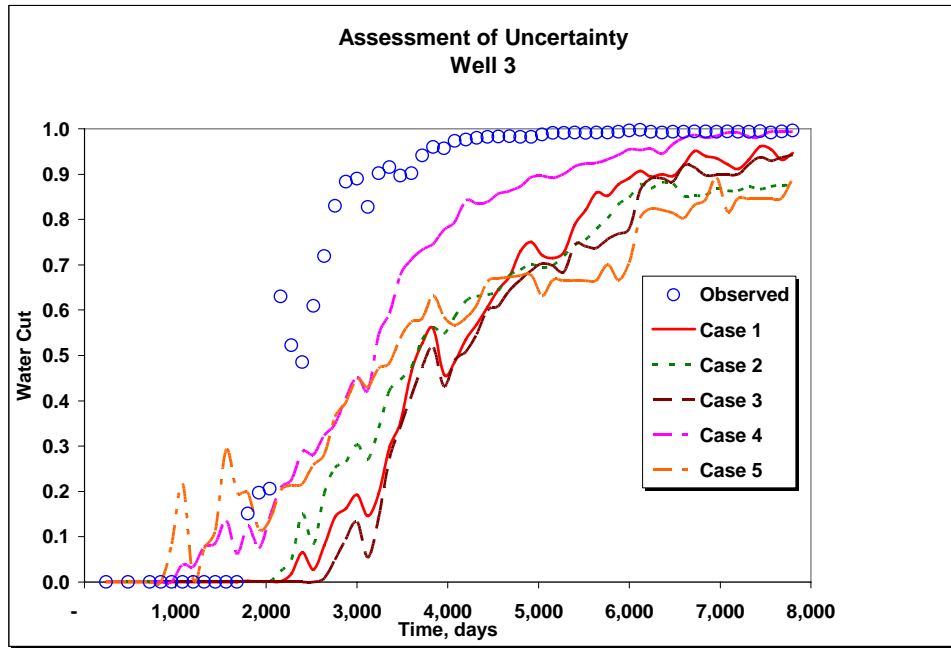


(a)

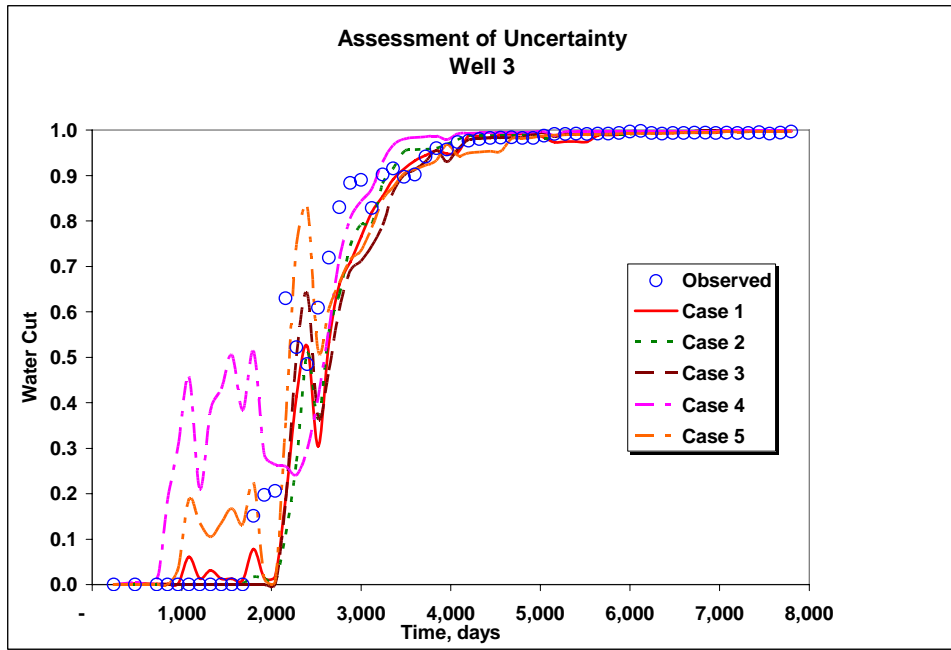


(b)

Fig. 4.4b – Water cut for well 2, CSGs. (a) Unconditioned, (b) Conditioned

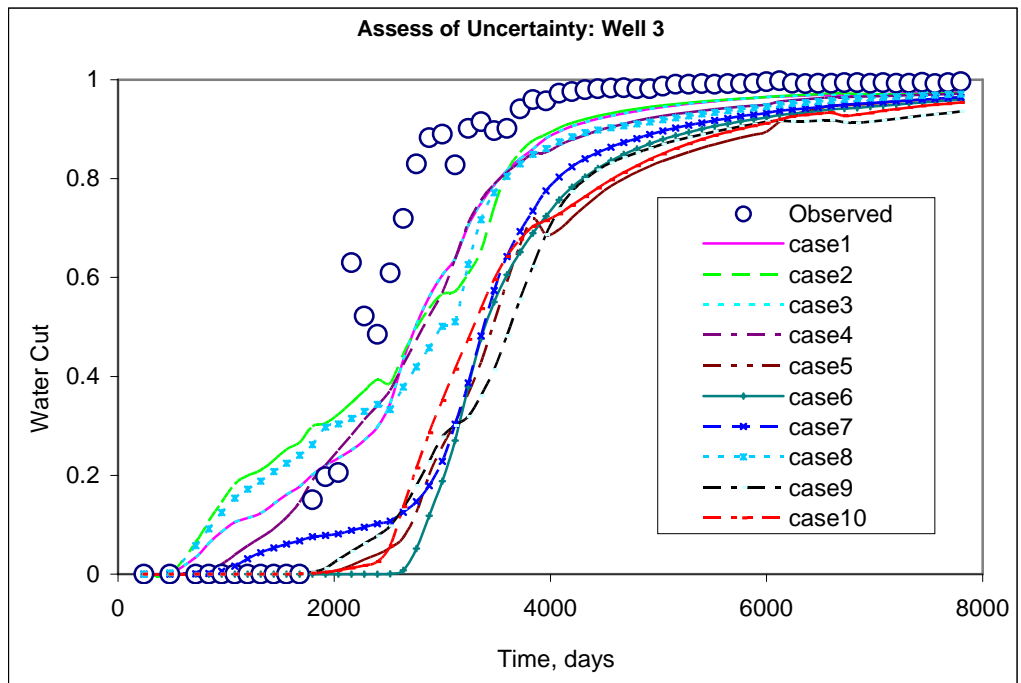


(a)

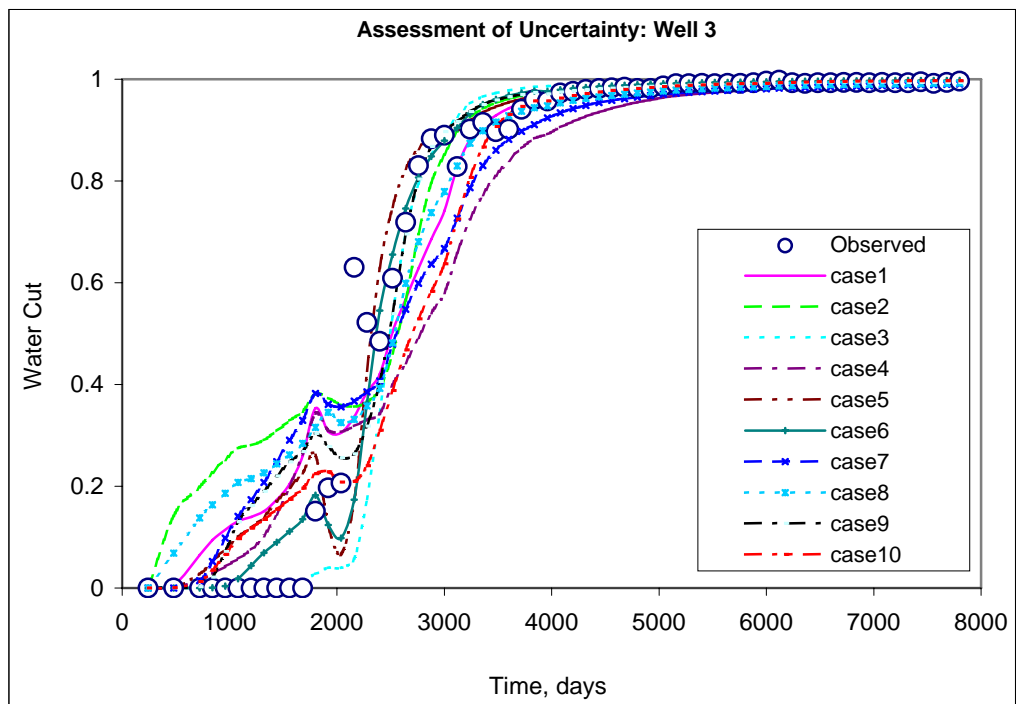


(b)

Fig. 4.5a – Water cut for well 3, Cloud Transform. (a) Unconditioned, (b) Conditioned

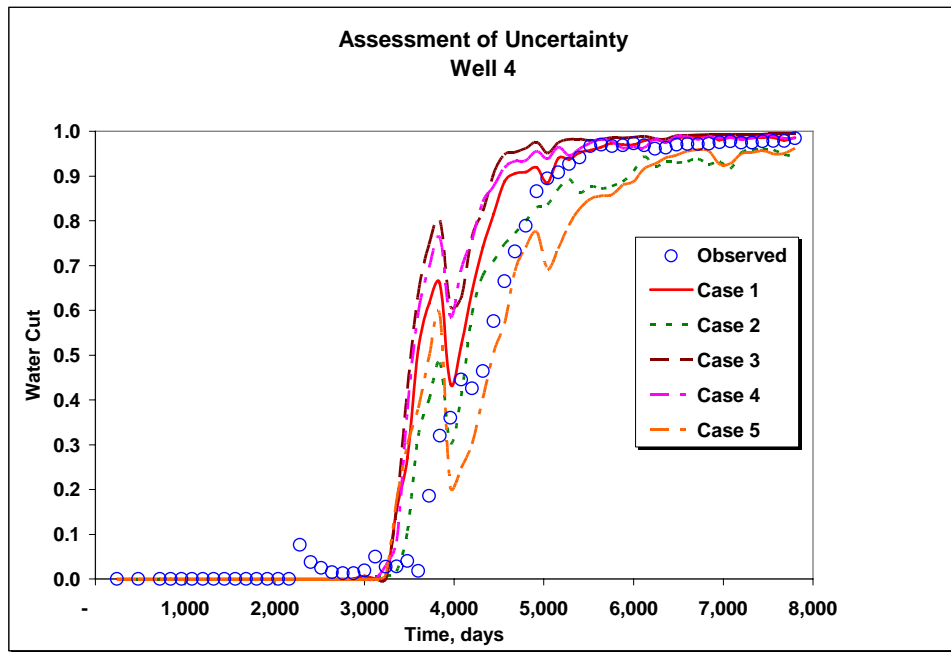


(a)

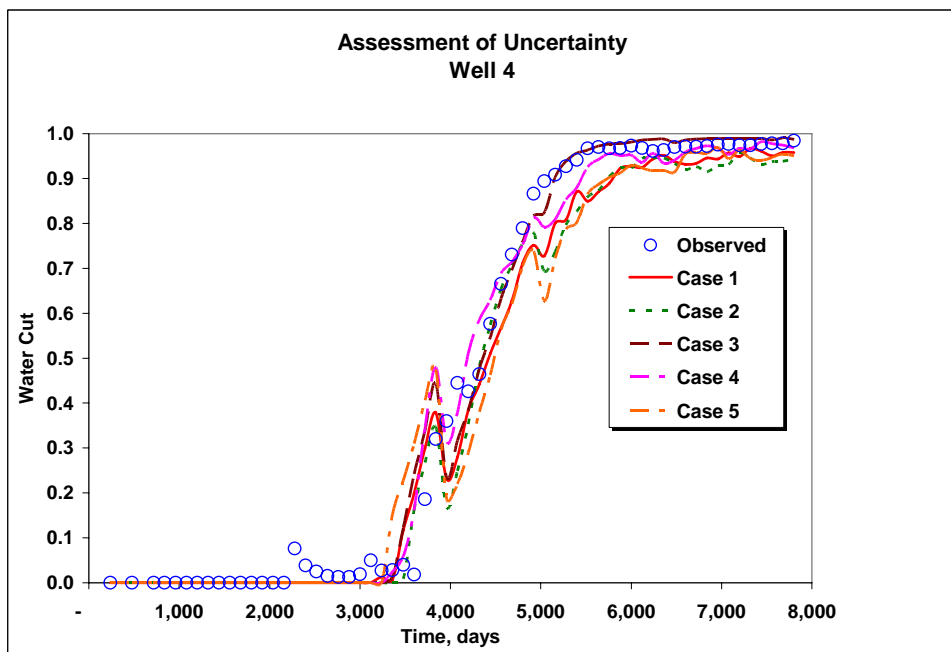


(b)

Fig. 4.5b – Water cut for well 3, CSGs. (a) Unconditioned, (b) Conditioned



(a)



(b)

Fig. 4.6a – Water cut for well 4, Cloud Transform. (a) Unconditioned, (b) Conditioned

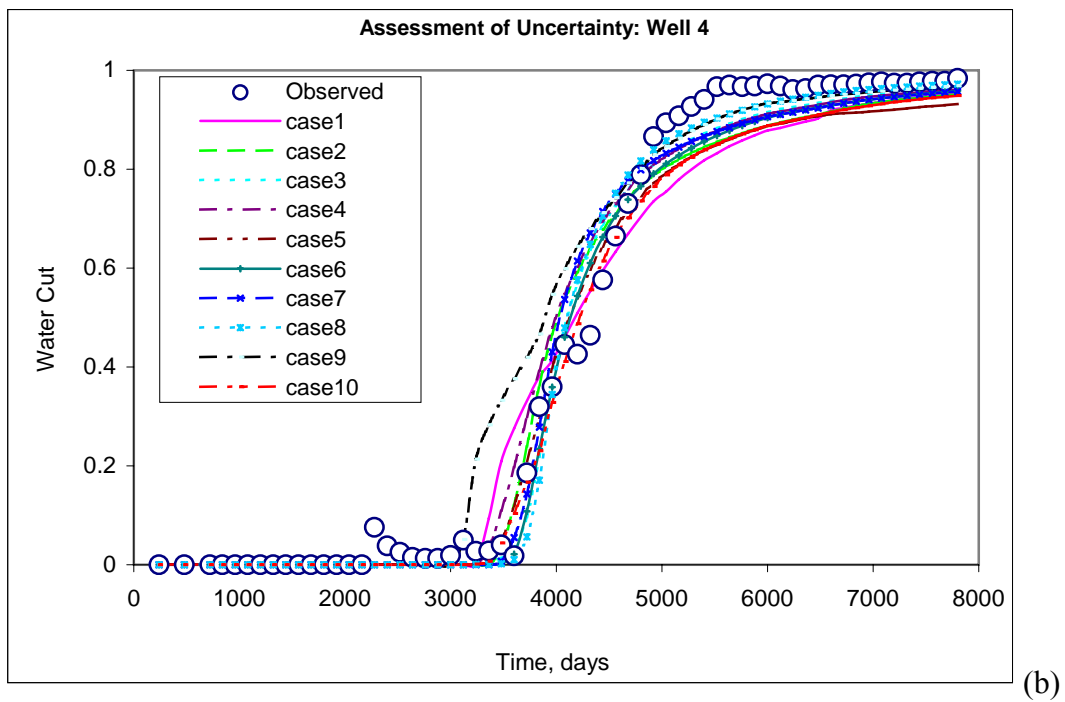
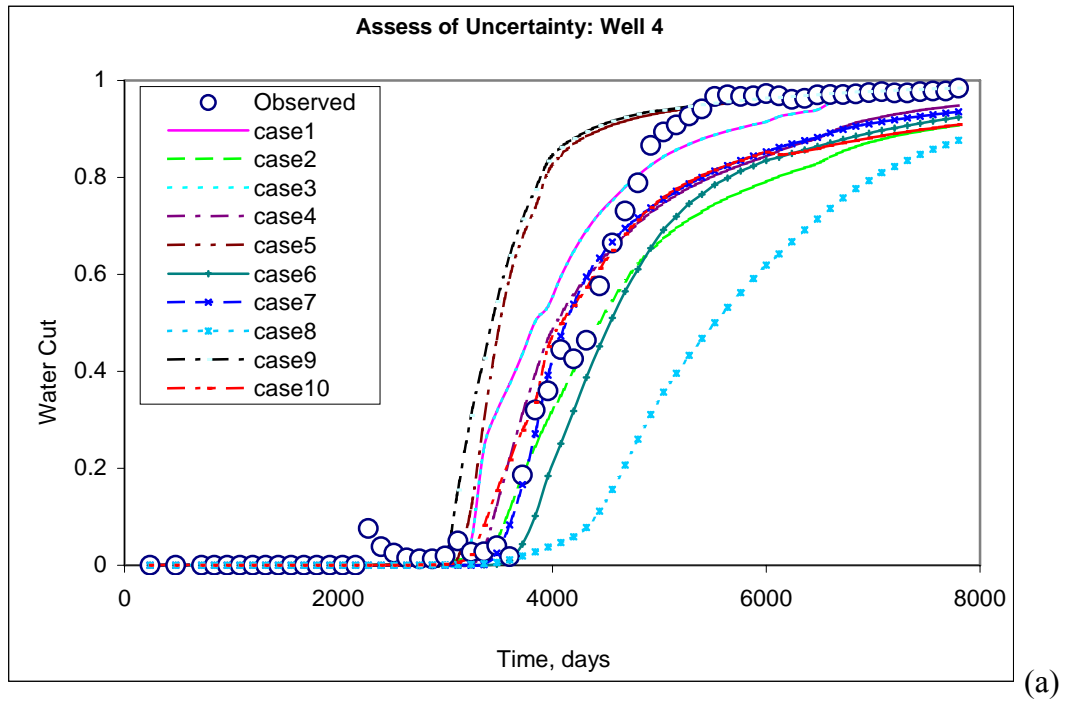


Fig. 4.6b – Water cut for well 4, CSGs. (a) Unconditioned, (b) Conditioned

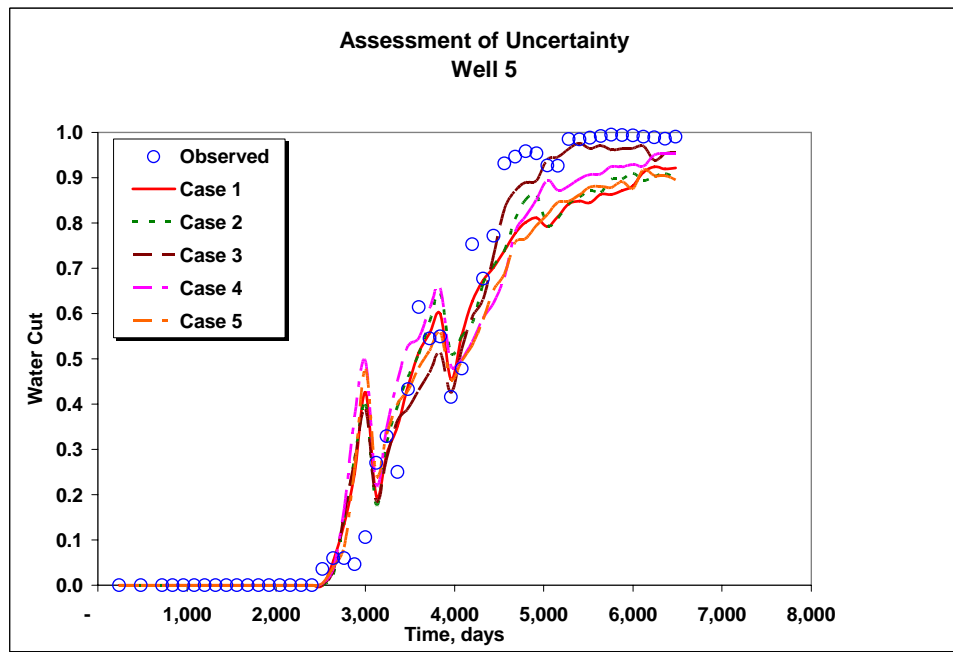
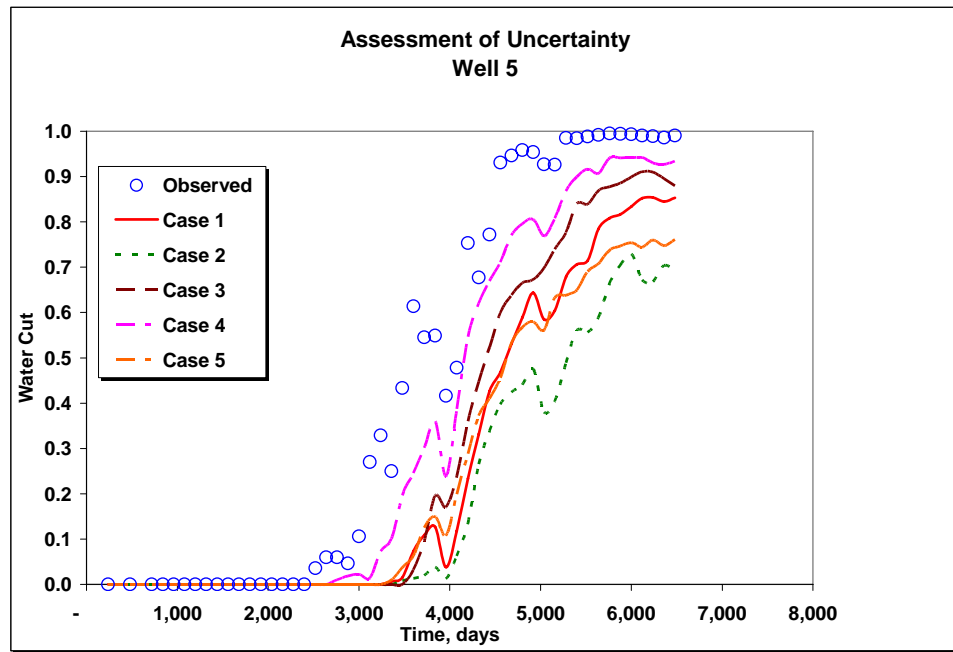
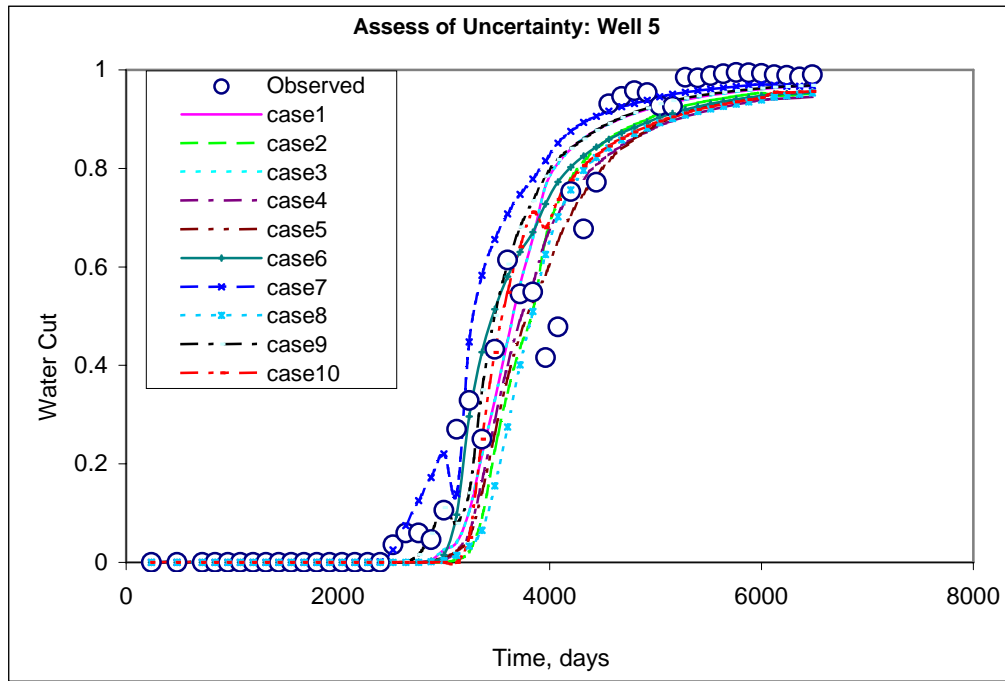
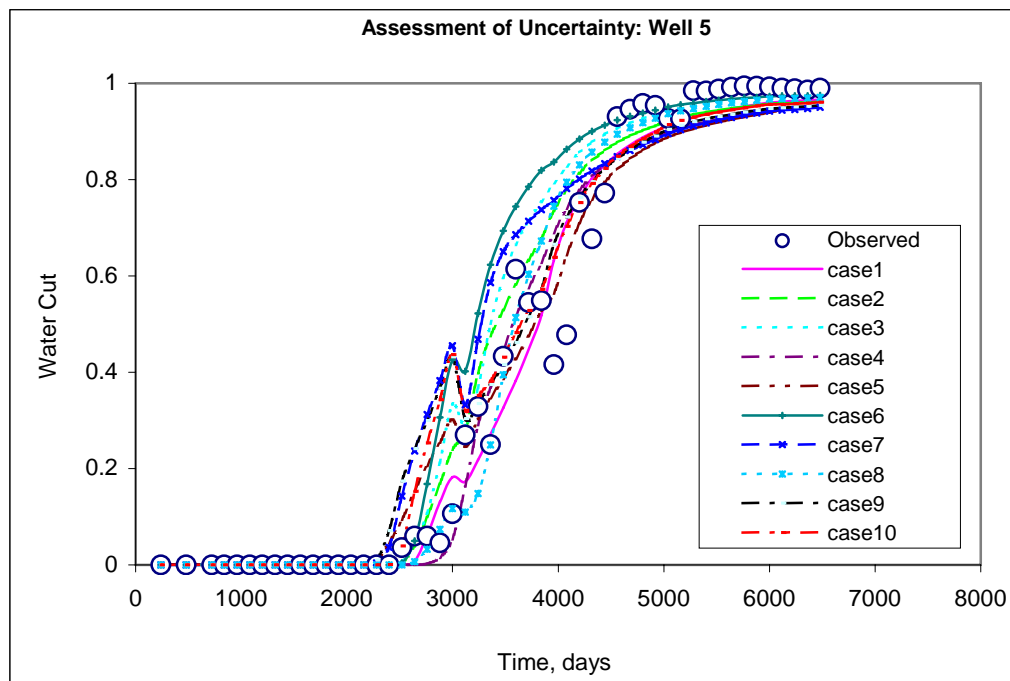


Fig. 4.7a – Water cut for well 5, Cloud Transform. (a) Unconditioned, (b) Conditioned

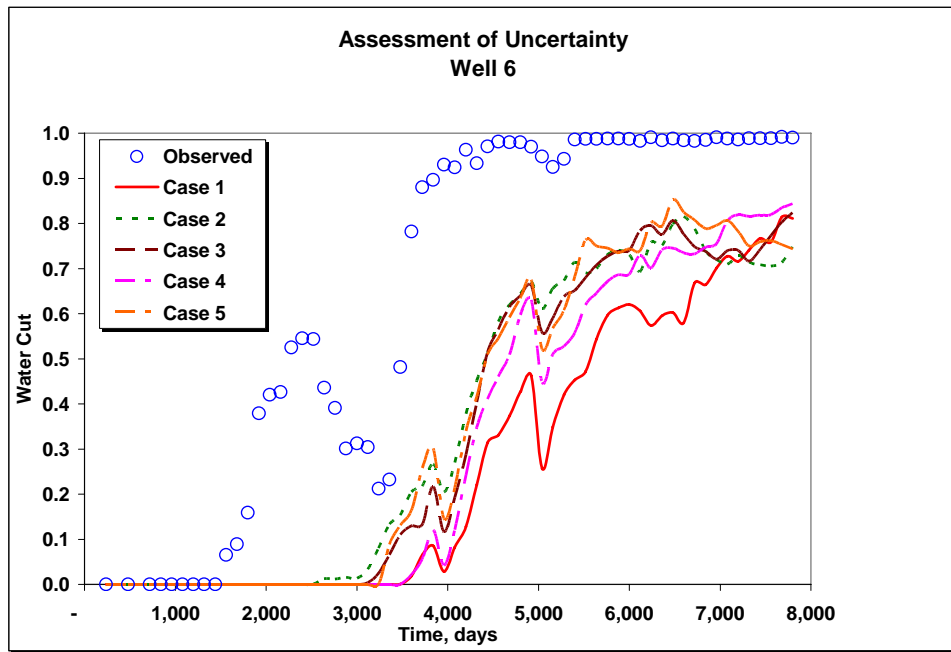


(a)

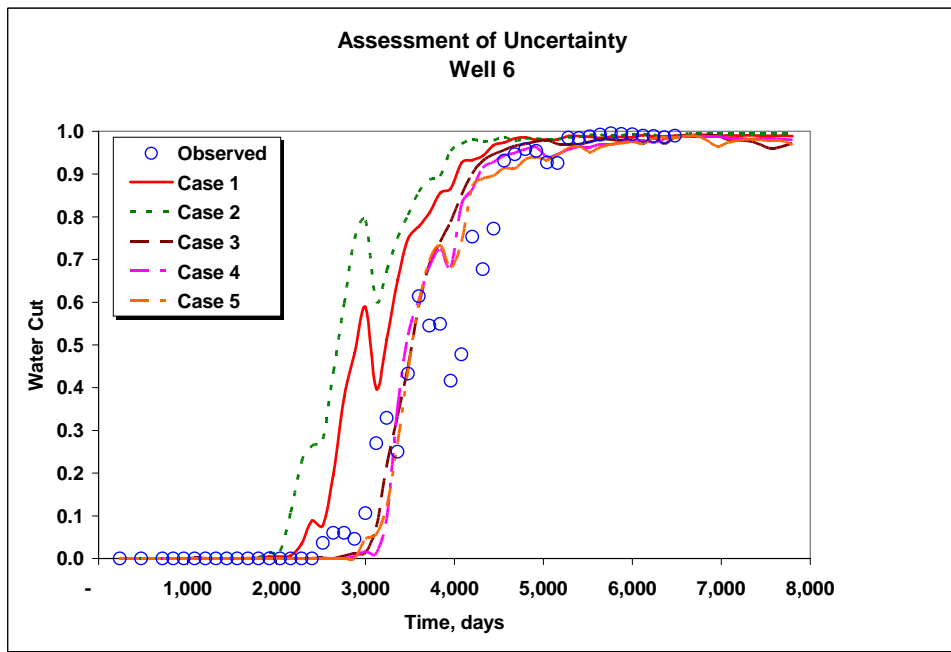


(b)

Fig. 4.7b – Water cut for well 5, CSGs. (a) Unconditioned, (b) Conditioned



(a)



(b)

Fig. 4.8a – Water cut for well 6, Cloud Transform. (a) Unconditioned, (b) Conditioned

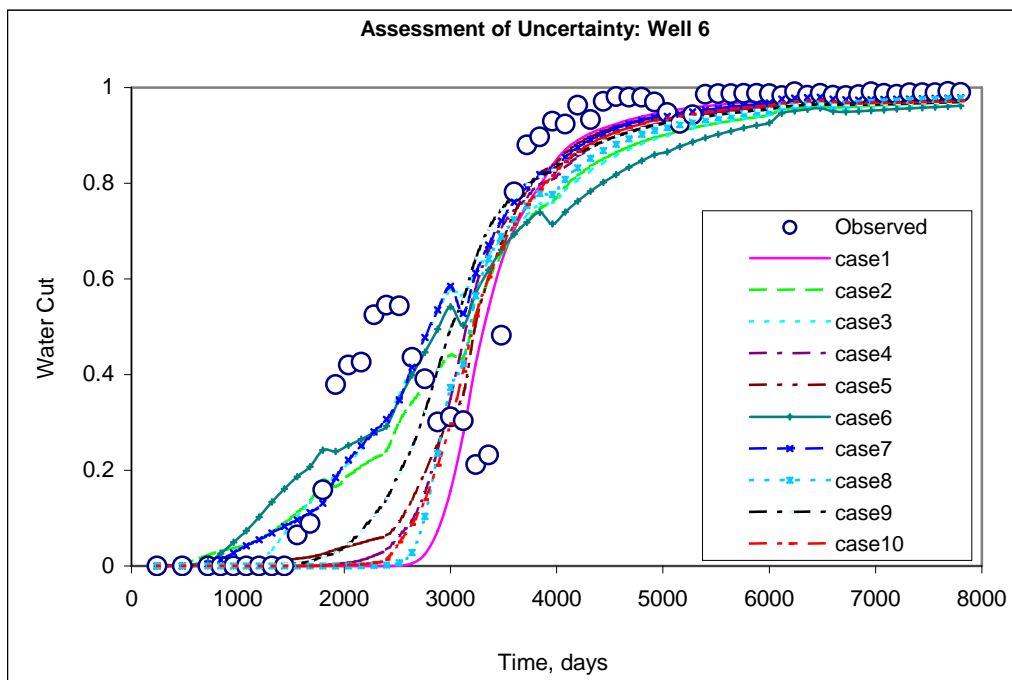
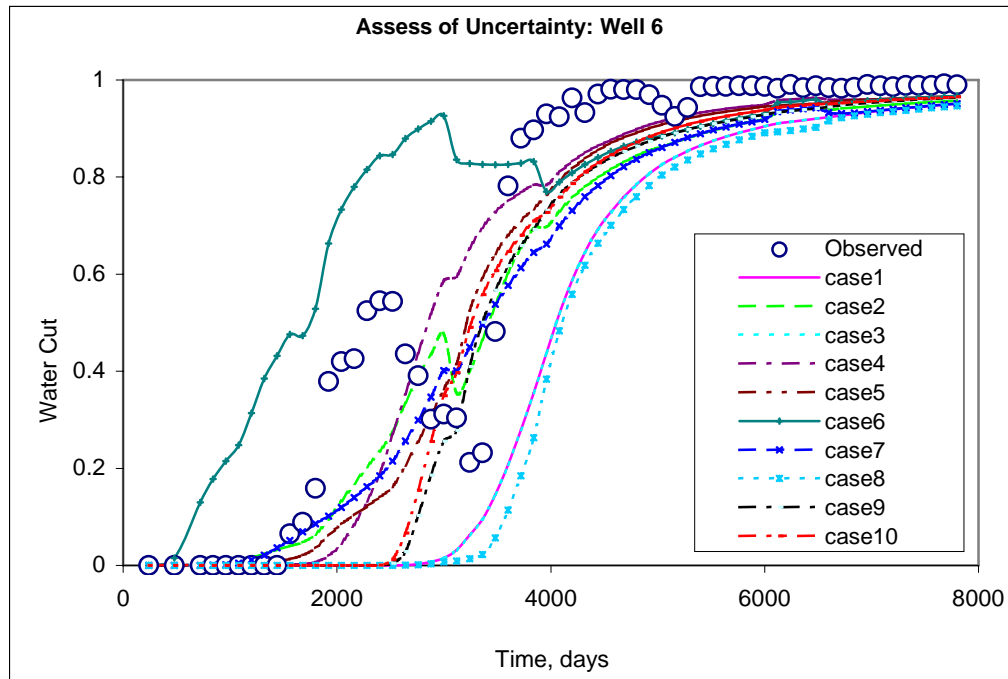
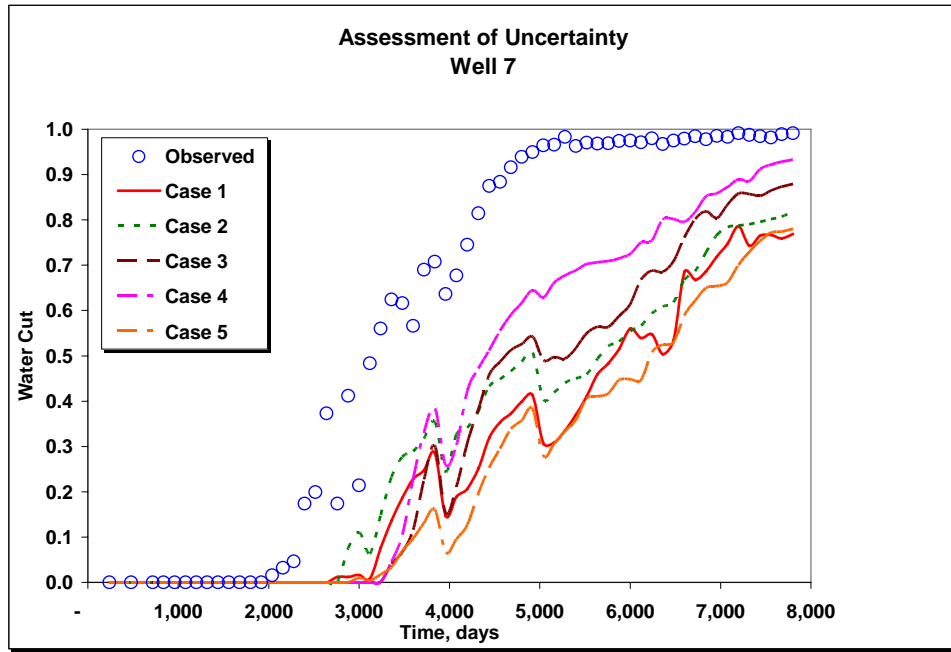
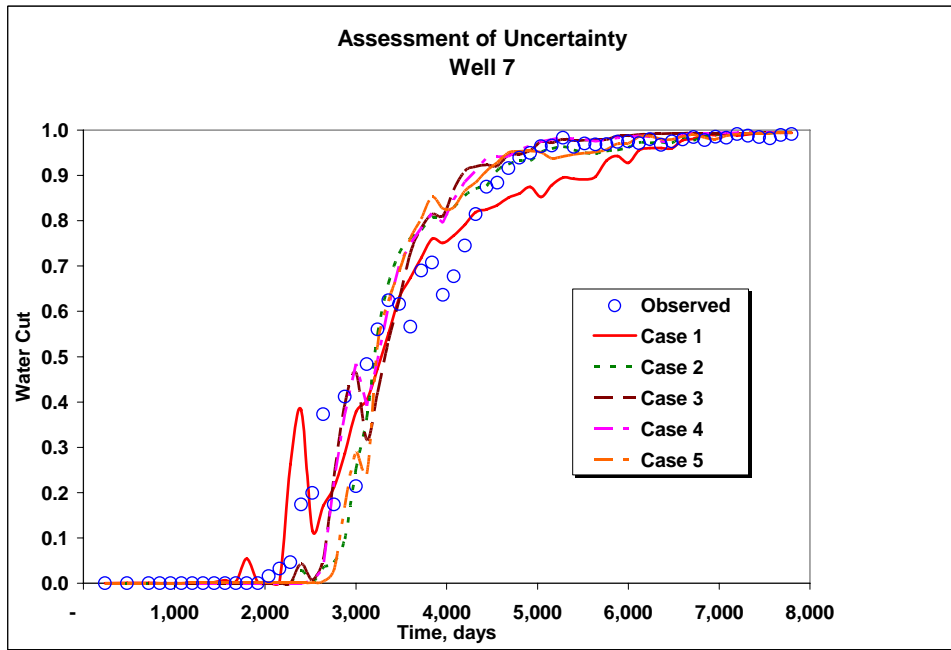


Fig. 4.8b – Water cut for well 6, CSGs. (a) Unconditioned, (b) Conditioned



(a)



(b)

Fig. 4.9a – Water cut for well 7, Cloud Transform. (a) Unconditioned, (b) Conditioned

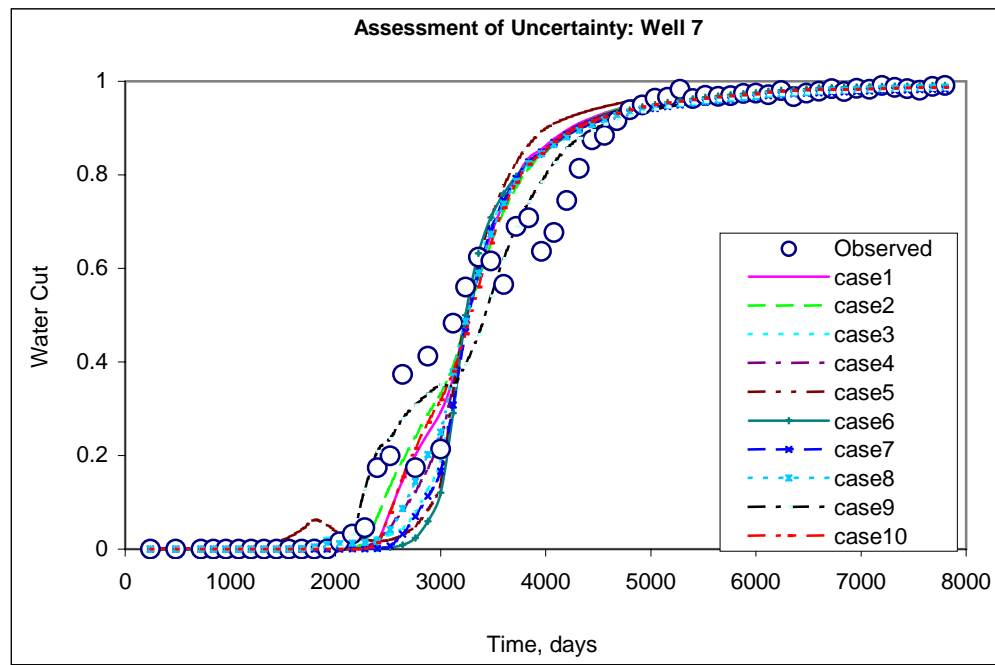
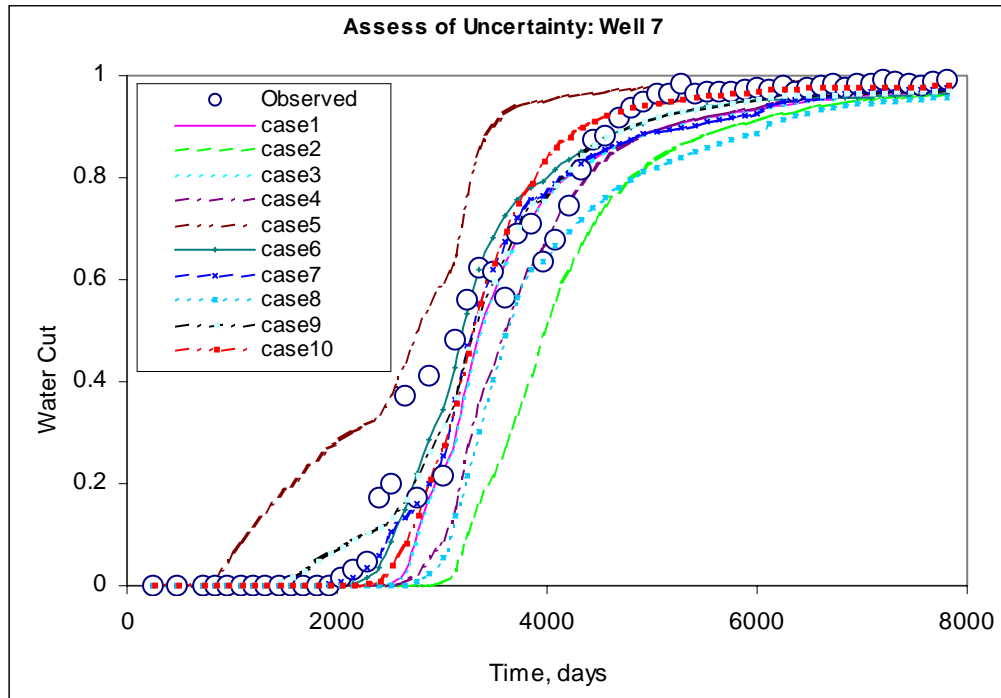


Fig. 4.9b – Water cut for well 7, CSGS. (a) Unconditioned, (b) Conditioned

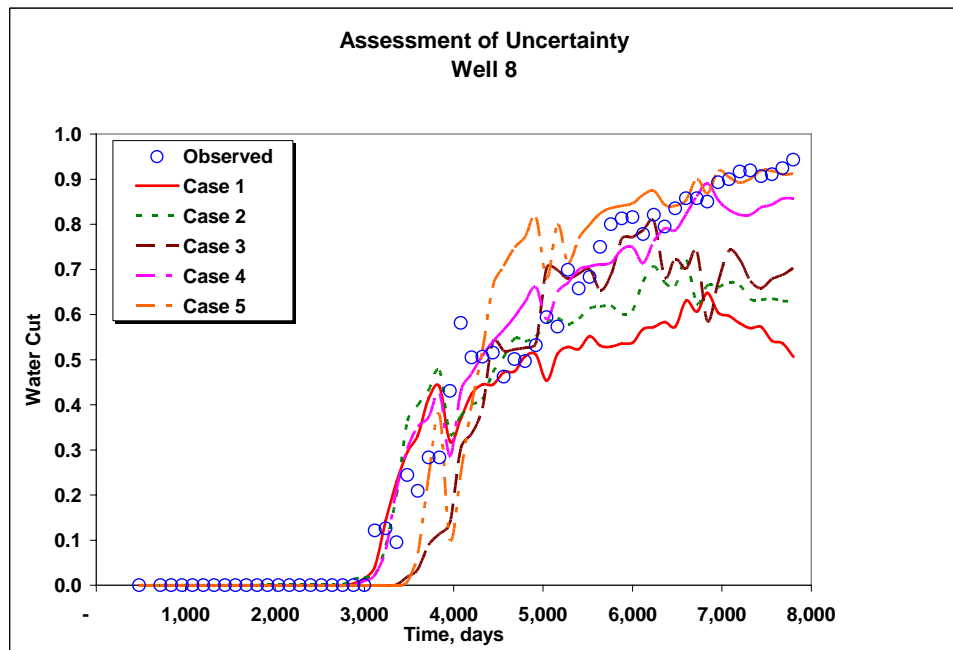
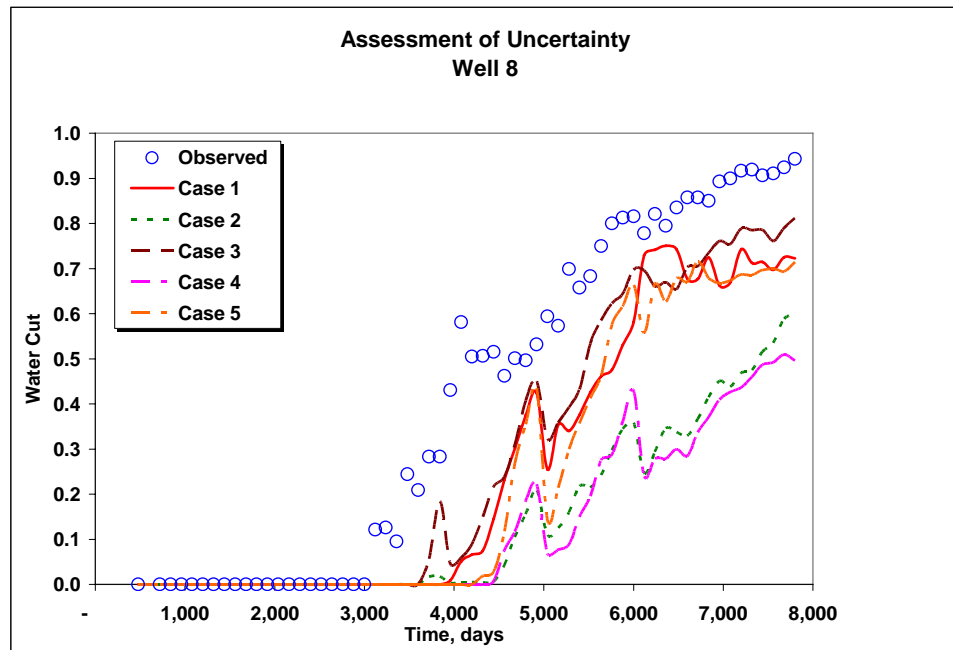


Fig. 4.10a – Water cut for well 8, Cloud Transform. (a) Unconditioned, (b) Conditioned

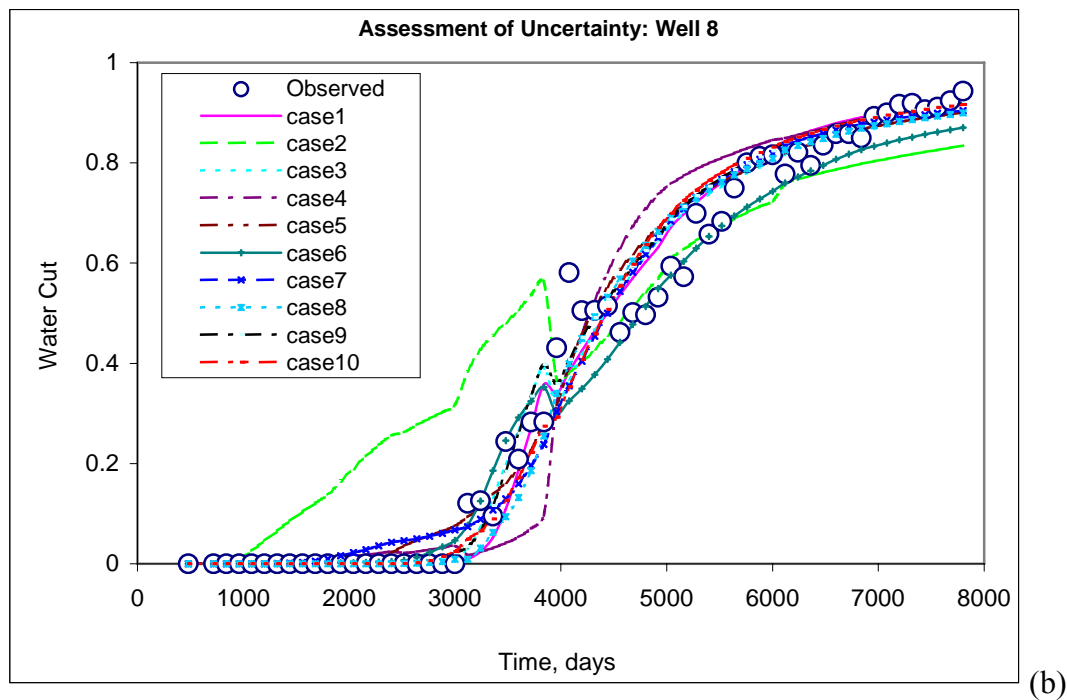
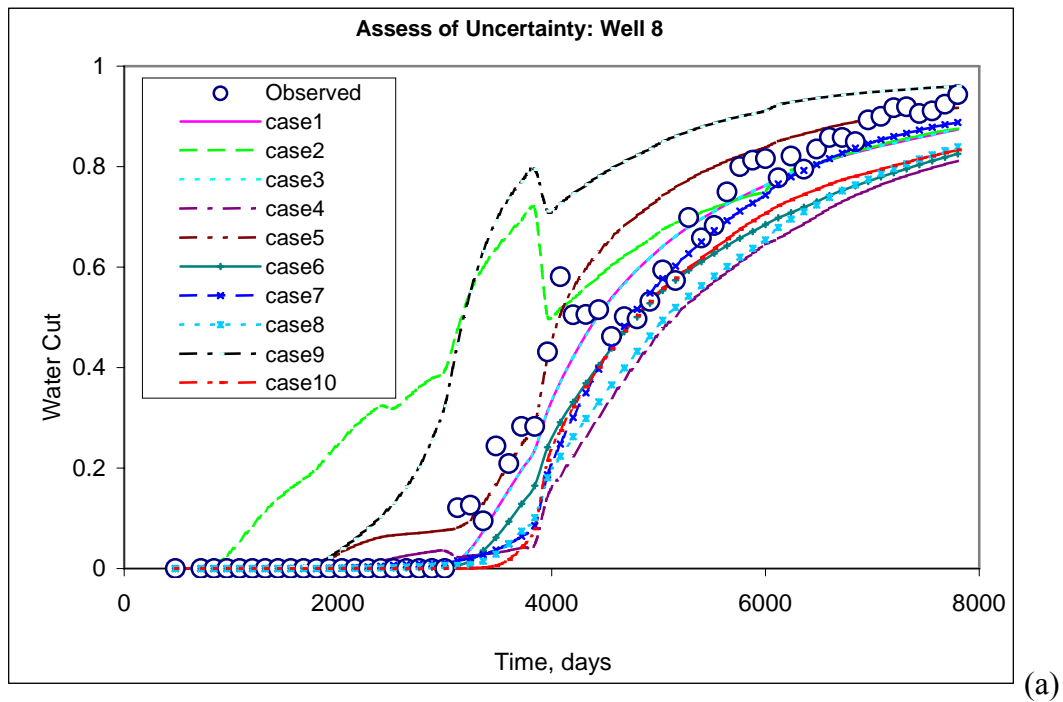


Fig. 4.10b – Water cut for well 8, CSGs. (a) Unconditioned, (b) Conditioned

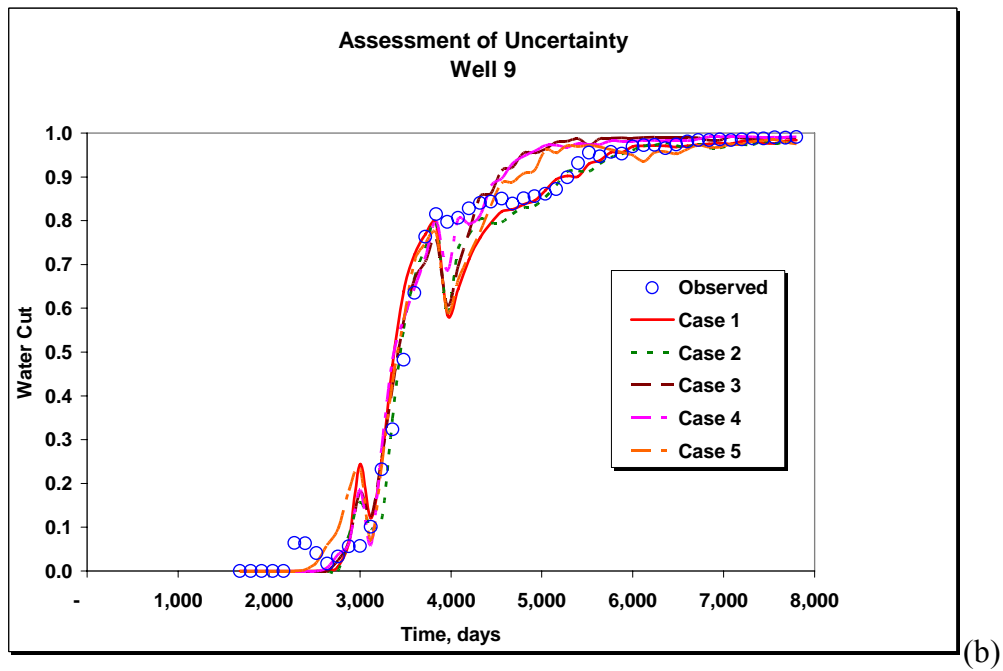
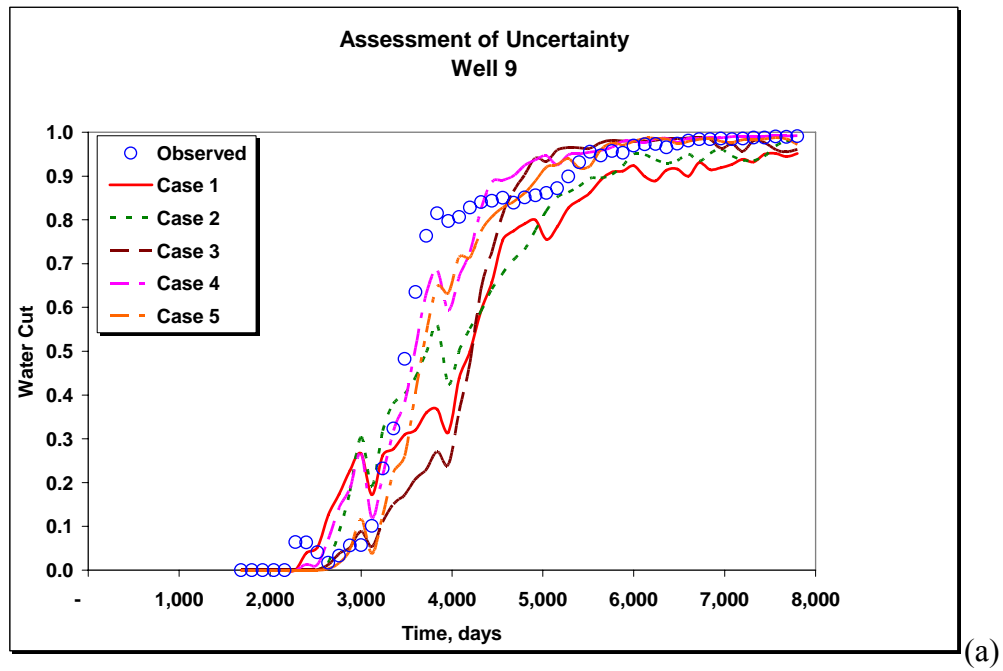
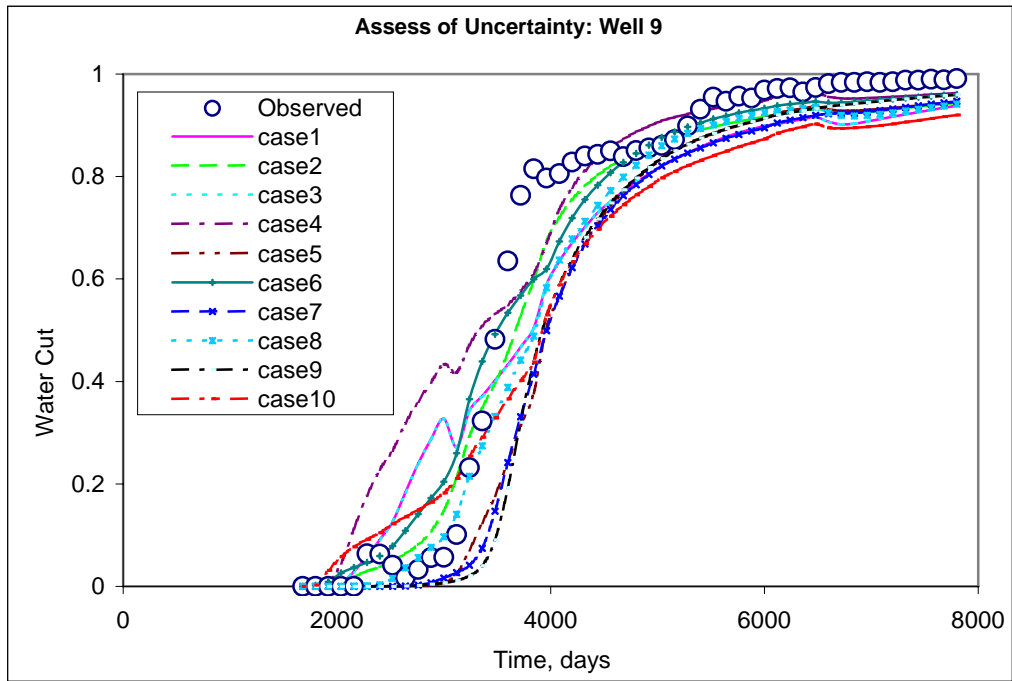
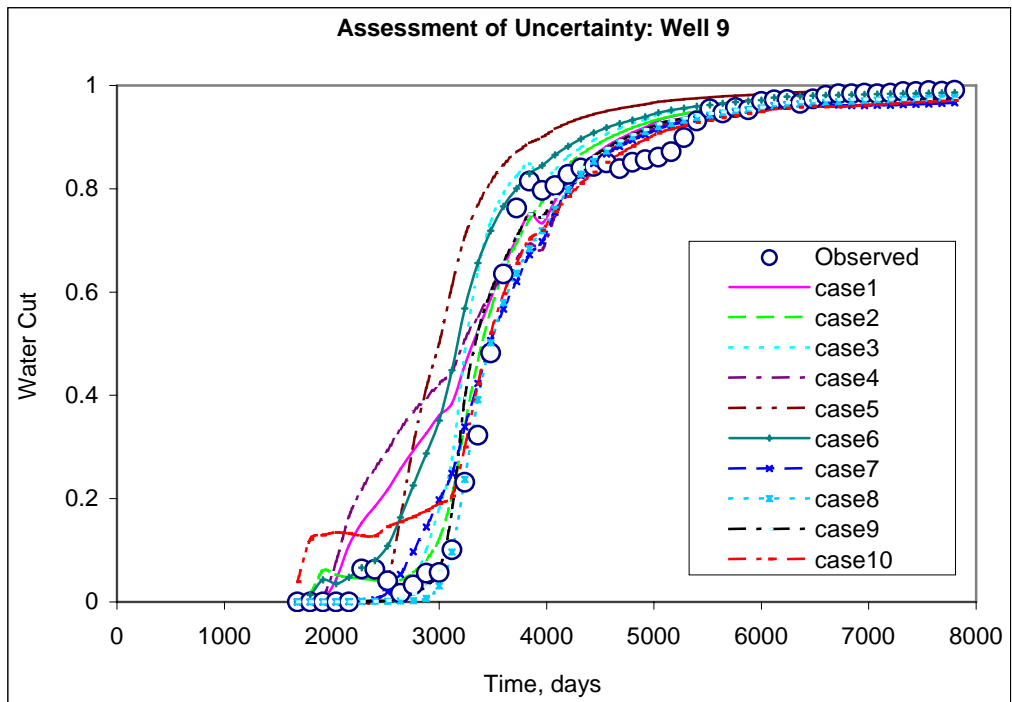


Fig. 4.11a – Water cut for well 9, Cloud Transform. (a) Unconditioned, (b) Conditioned



(a)



(b)

Fig. 4.11b – Water cut for well 9, CSGs. (a) Unconditioned, (b) Conditioned

4.4 Uncertainty Assessment in Prediction of Performance

It could be shown with the field application that a quantitative measure of the change in uncertainty resulting from the integration of production data was feasible. However, sound match does not ensure a sound prediction based on the nature of non-uniqueness and difficulties to completely sample from the posterior. A more practical application would be to be able to condition the reservoir model using limited production data to then predict future reservoir performance. The scatter in the ensemble of predictive water cut curves would thus provide an uncertainty assessment tool. The comparison of prediction with available data will be an indicator of the quality of the approach applied.

The entire available data are 7800-day water cut data. First half data of about 4000 days are integrated with unconditioned permeability and water cut data, the efficient Bayesian formulation described in Chapter II are used. The prior model by cloud transform and collocated simulation are integrated with water cut respectively.

The conditioned water cut is shown as **Figs. 4.12 to 4.20** for prior modeling by Cloud Transform.

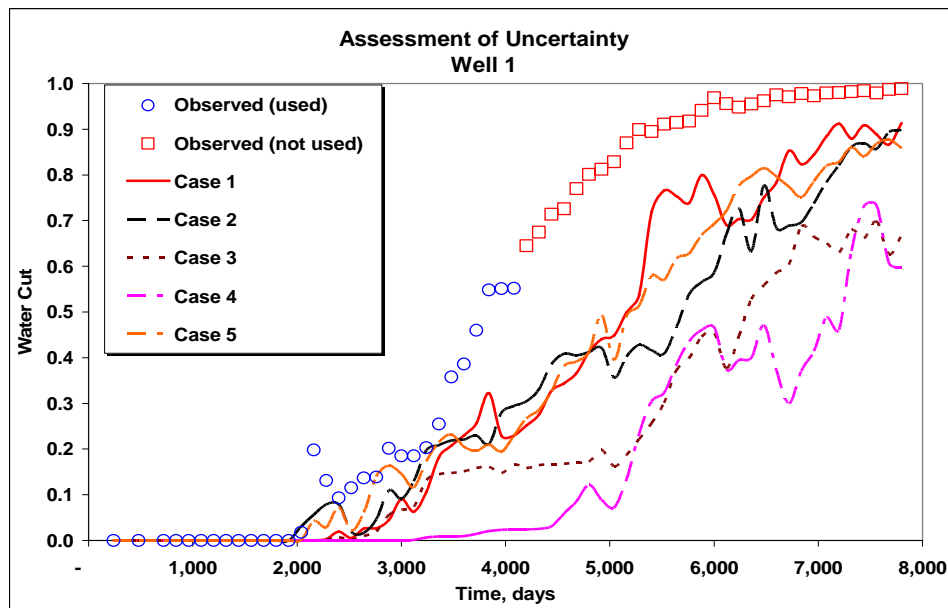
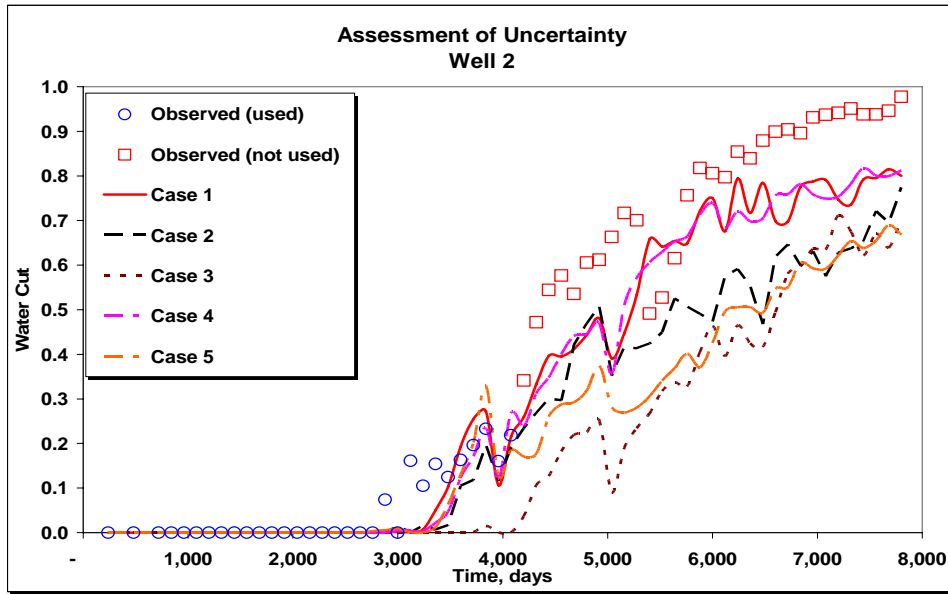
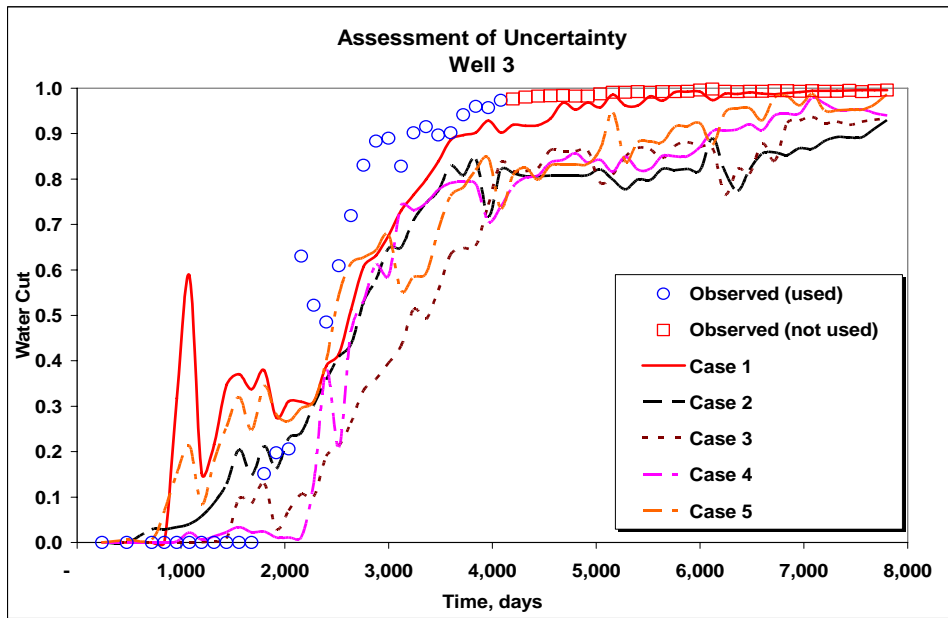


Fig. 4.12 – Conditioned water cut for well 1, Cloud Transform
Using 4,080 days data, Prediction to 7,800 days



**Fig. 4.13 – Conditioned water cut for well 2, Cloud Transform
Using 4,080 days data, Prediction to 7,800 days**



**Fig. 4.14 – Conditioned water cut for well 3, Cloud Transform
Using 4,080 days data, Prediction to 7,800 days**

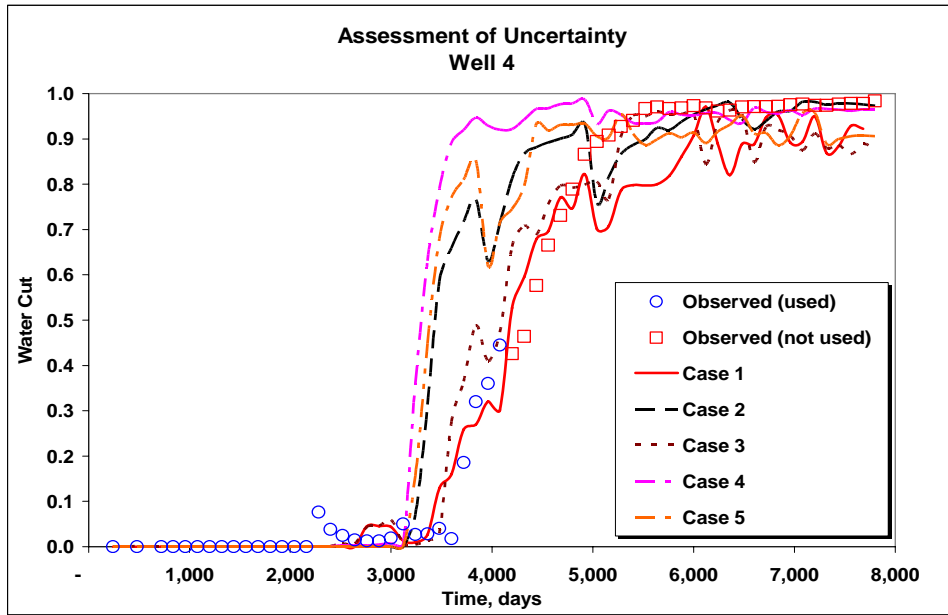


**Fig. 4.15 – Conditioned water cut for well 4, Cloud Transform
Using 4,080 days data, Prediction to 7,800 days**

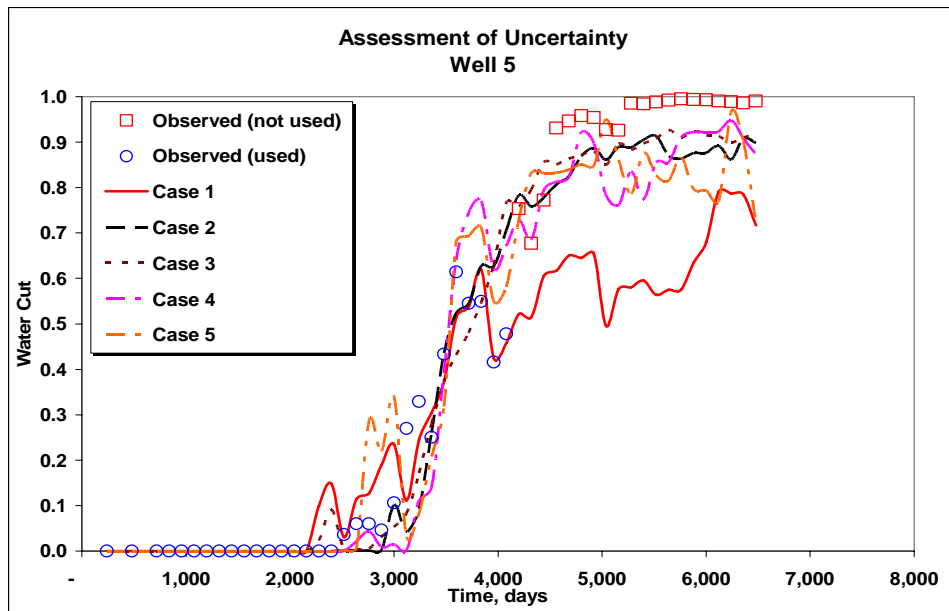


**Fig. 4.16 – Conditioned water cut for well 5, Cloud Transform
Using 4,080 days data, Prediction to 7,800 days**

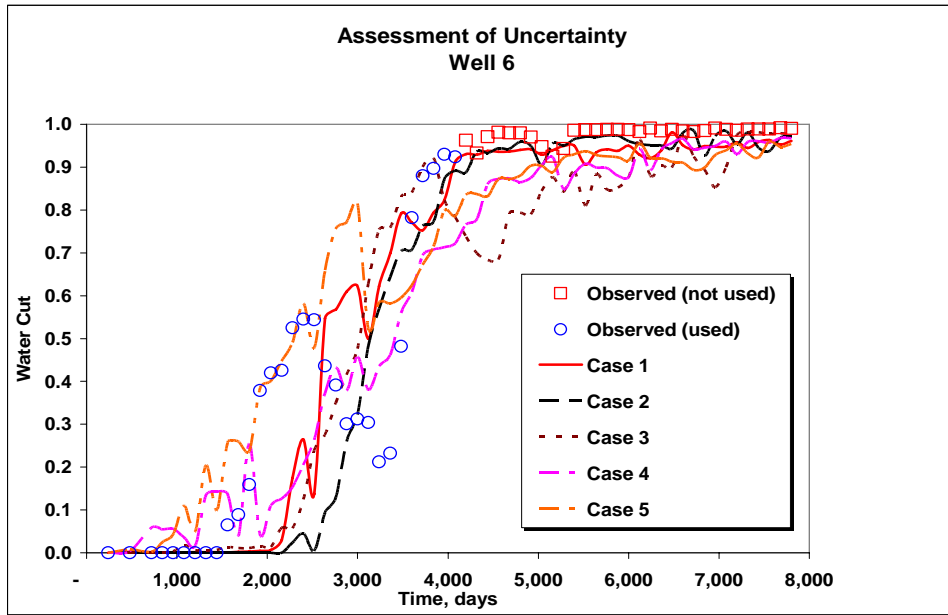


**Fig. 4.17 – Conditioned water cut for well 6, Cloud Transform
Using 4,080 days data, Prediction to 7,800 days**

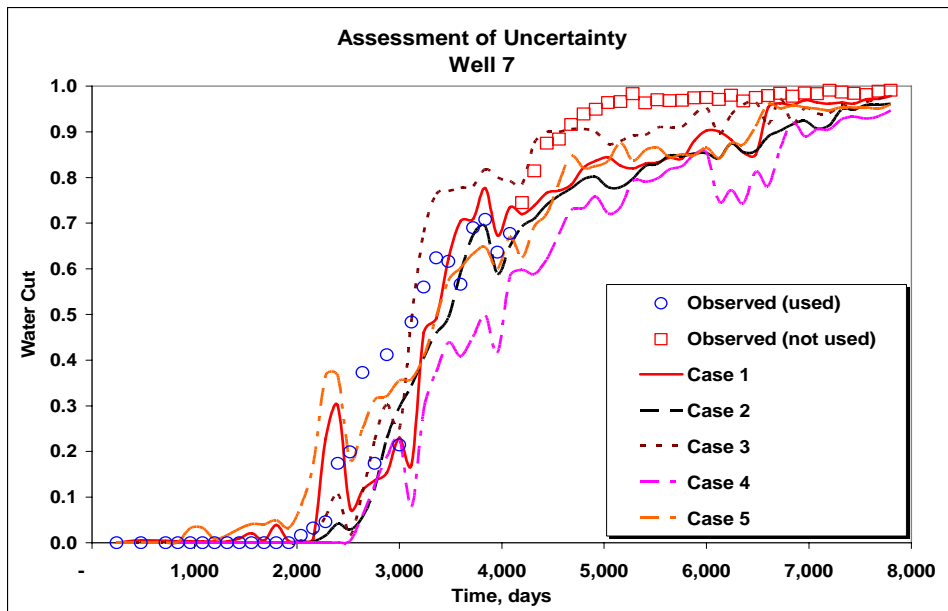


**Fig. 4.18 – Conditioned water cut for well 7, Cloud Transform
Using 4,080 days data, Prediction to 7,800 days**

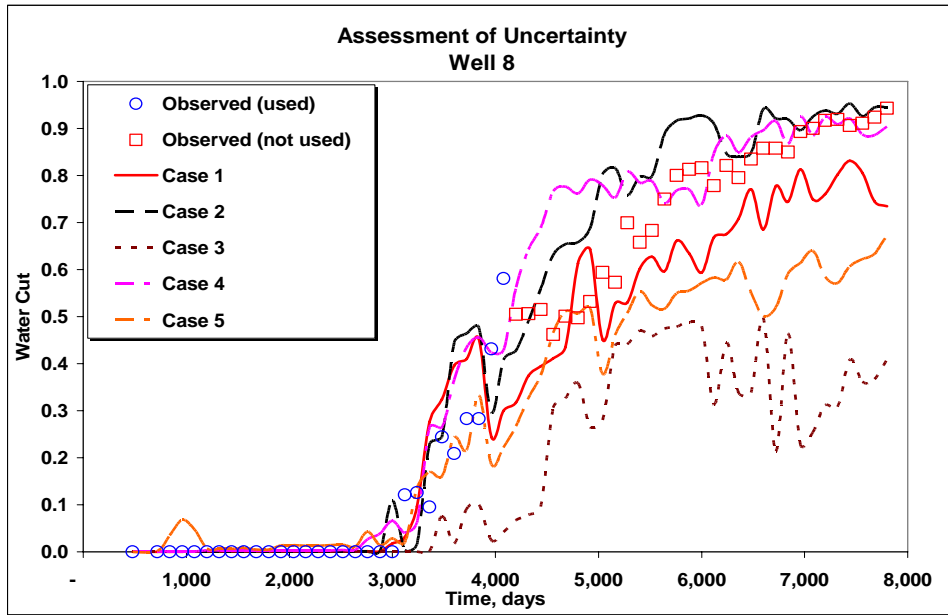


**Fig. 4.19 – Conditioned water cut for well 8, Cloud Transform
Using 4,080 days data, Prediction to 7,800 days**

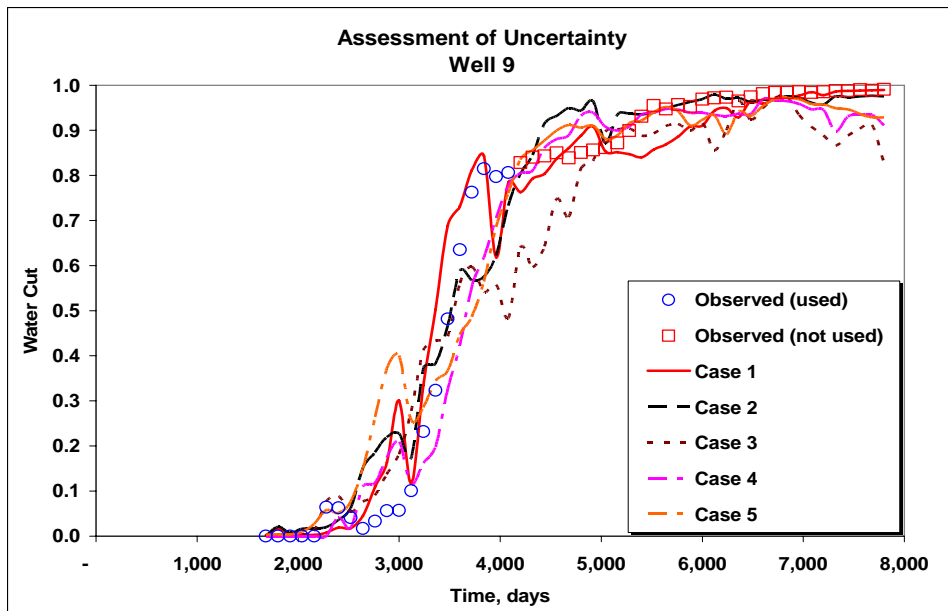


**Fig. 4.20 – Conditioned water cut for well 9, Cloud Transform
Using 4,080 days data, Prediction to 7,800 days**

The conditioned water cut is shown as **Figs. 4.21 to 4.29** for CSGs method.

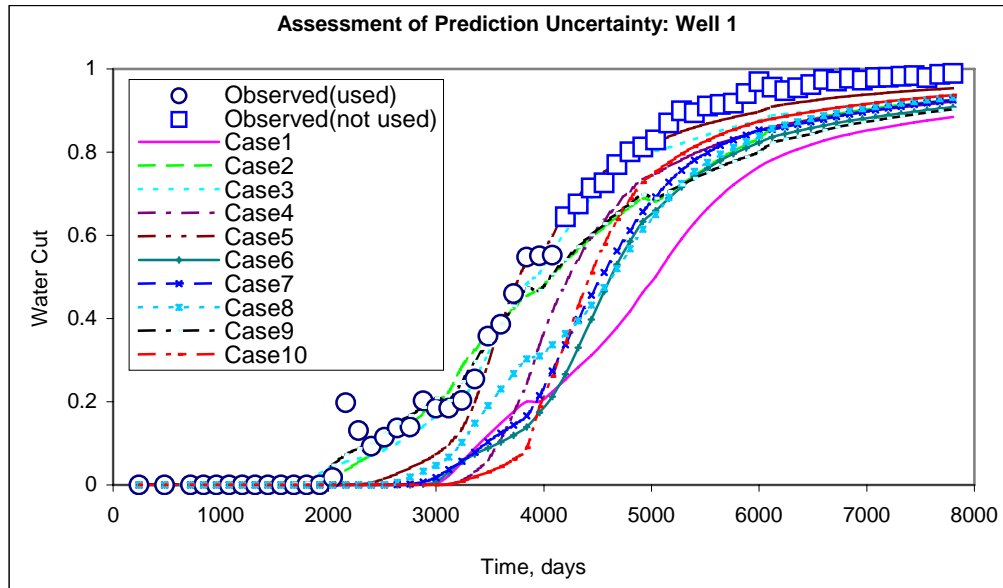


Fig. 4.21 – Conditioned water cut for well 1, Collocated SGS
Using 4,080 days data, Prediction to 7,800 days

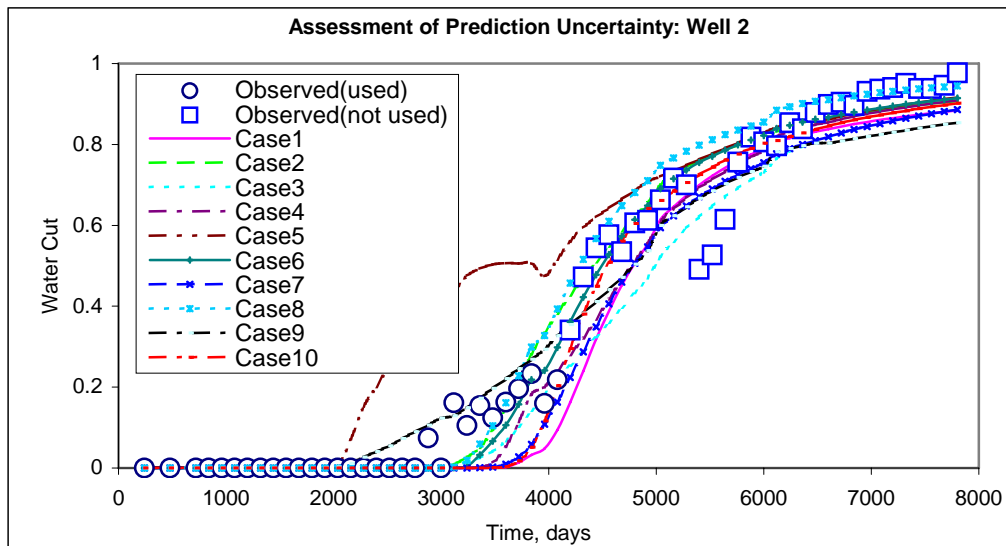
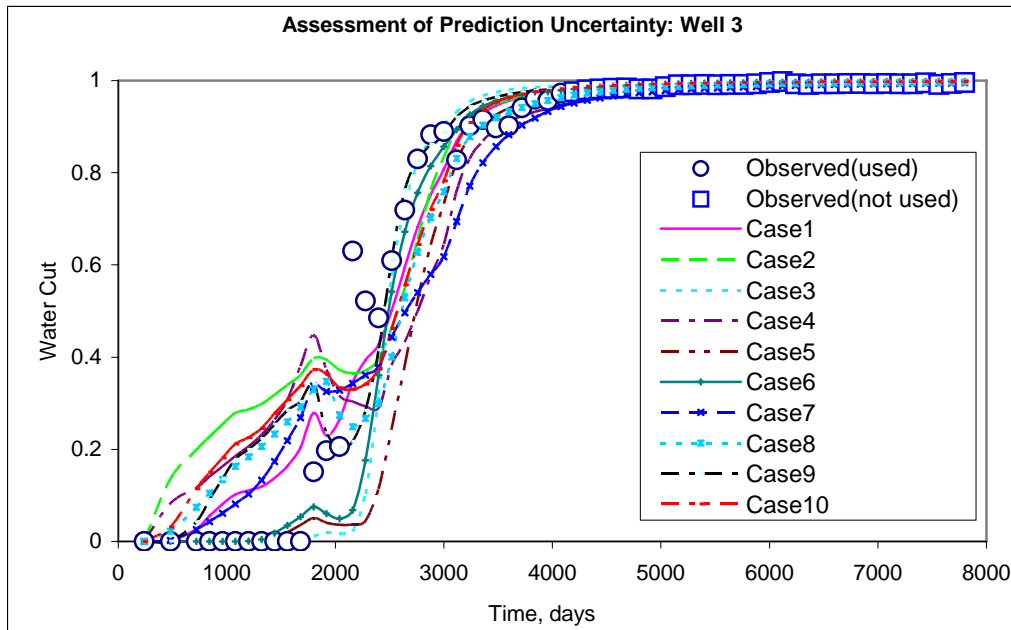
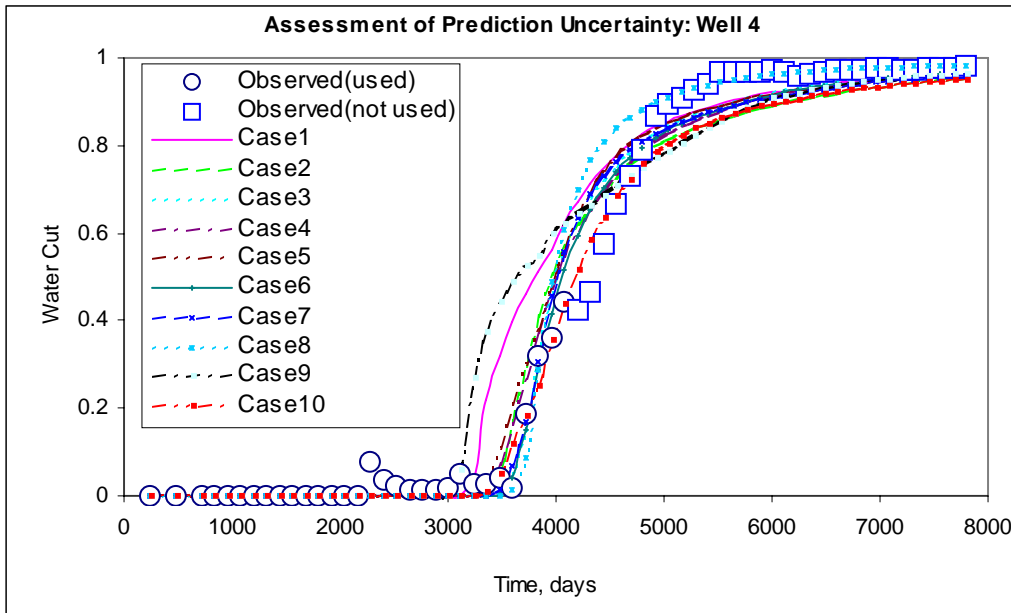


Fig. 4.22 – Conditioned water cut for well 2, Collocated SGS
Using 4,080 days data, Prediction to 7,800 days



**Fig. 4.23 – Conditioned water cut for well 3, Collocated SGS
Using 4,080 days data, Prediction to 7,800 days**



**Fig. 4.24 – Conditioned water cut for well 4, Collocated SGS
Using 4,080 days data, Prediction to 7,800 days**

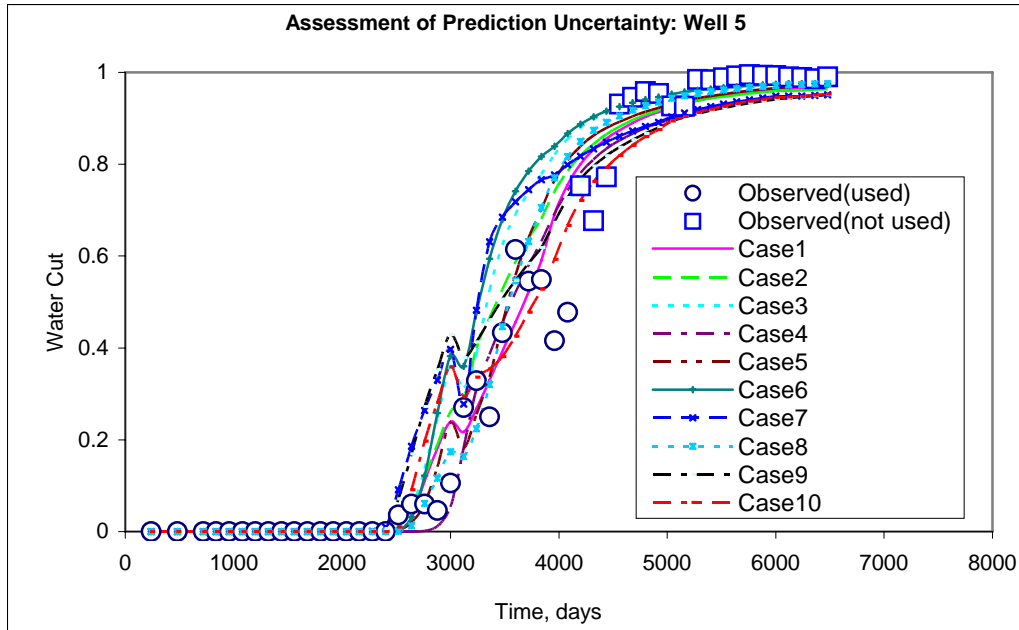


**Fig. 4.25 – Conditioned water cut for well 5, Collocated SGS
Using 4,080 days data, Prediction to 7,800 days**

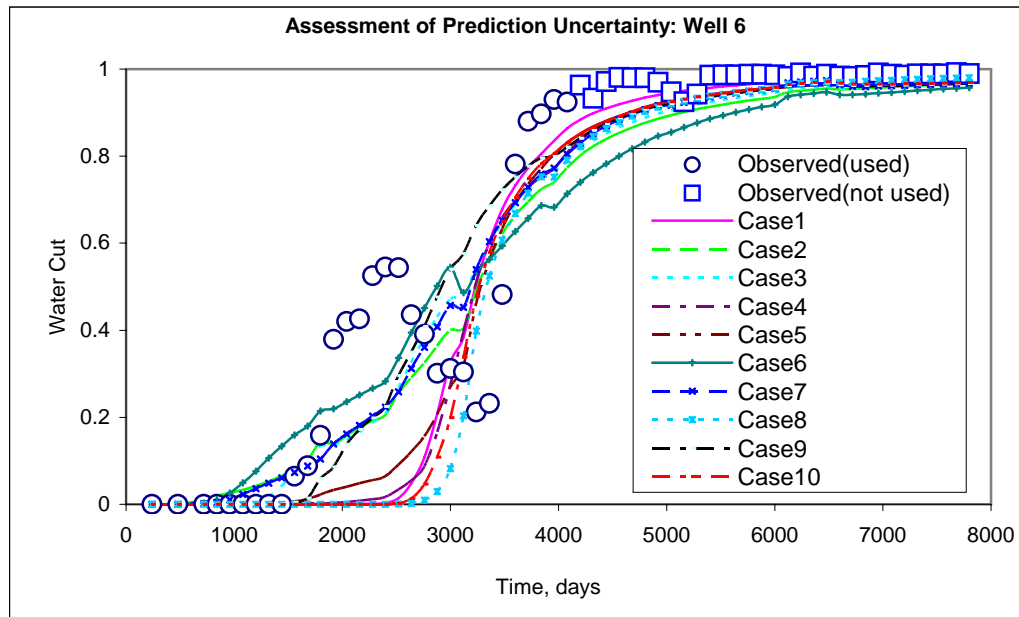


**Fig. 4.26 – Conditioned water cut for well 6, Collocated SGS
Using 4,080 days data, Prediction to 7,800 days**

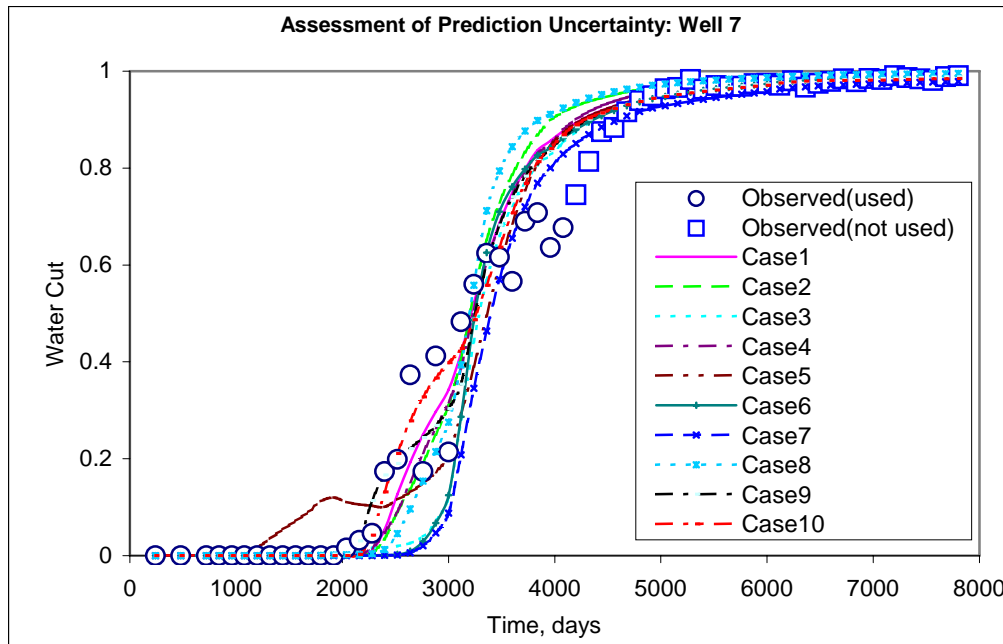


Fig. 4.27 – Conditioned water cut for well 7, Collocated SGS
 Using 4,080 days data, Prediction to 7,800 days

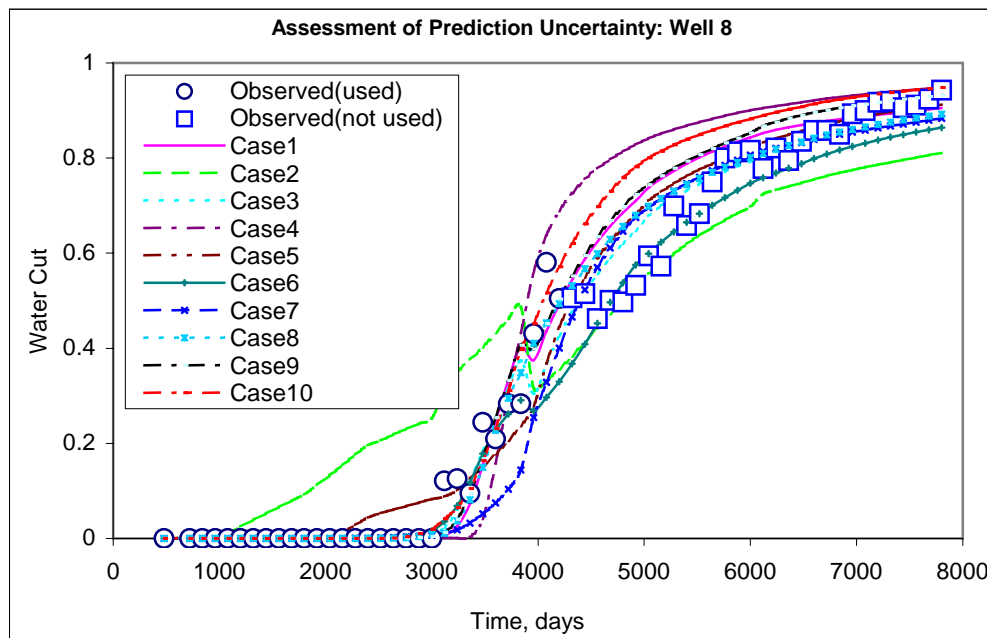
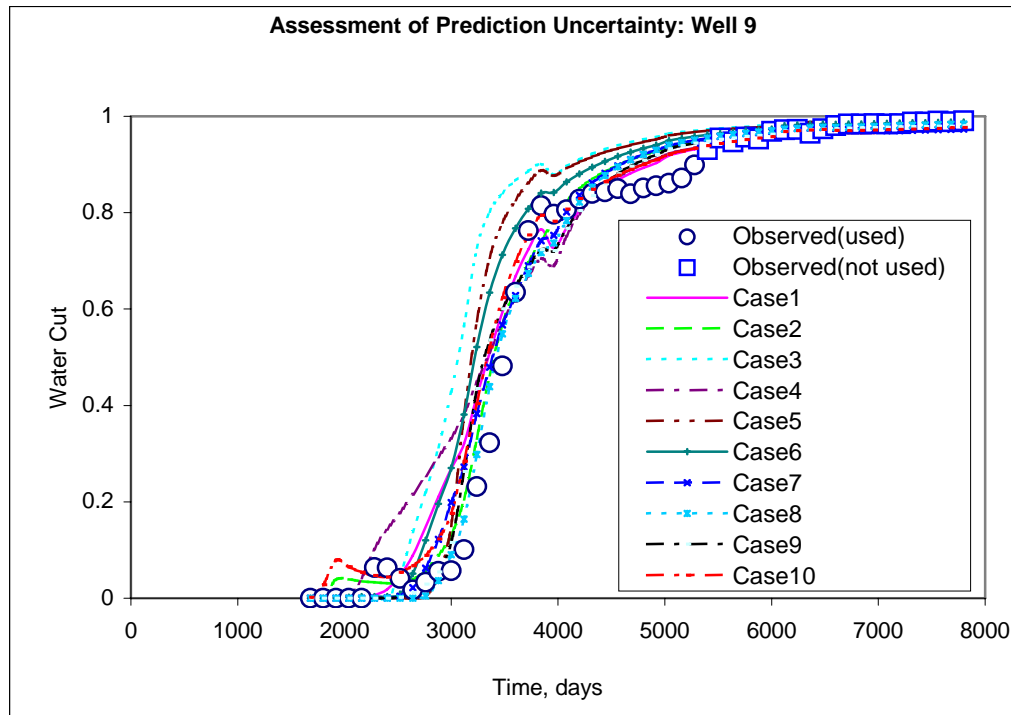


Fig. 4.28 – Conditioned water cut for well 8, Collocated SGS
 Using 4,080 days data, Prediction to 7,800 days



**Fig. 4.29 – Conditioned water cut for well 9, Collocated SGS
Using 4,080 days data, Prediction to 7,800 days**

After comparing the spread in the posteriors from prior modeling by cloud transform and Collocated Sequential Gaussian Simulation, we can see the spread in the prior modeling will influence the spread in the matching and prediction of data.

By the Collocated Sequential Gaussian Simulation, the prior distribution of permeability field is better modeled than that from cloud transform. The explanation is that, in Collocated SGS, the information of spatial relation among prior data is integrated by modeling of the covariance matrix of them while in the cloud transform, no information on spatial relation of permeability and porosity is included.

It is important to exhaust available quantified information in the priors before integration of dynamic data.

CHAPTER V

CONCLUSIONS AND RECOMMENDATIONS

Integration of production data and assessment of uncertainty by multiple realizations can be done by Bayesian approach. This inverse problem is computationally intensive for large-scale field case because sensitivity computations and conventional minimization algorithms have high computation costs.

5.1 Conclusions

We propose an adaptation of the Bayesian formulation, which can be solved efficiently by LSQR and along with other advantages that overcomes limitations of current approach.

(1) The advantages can be summarized in following.

a. Sensitivity Calculation.

It uses streamline-based analytic sensitivity Streamline-based sensitivity. The calculation of streamline sensitivity requires only one forward simulation and is applicable for both streamline and commercial finite-difference simulators.

b. Data Misfit Calculation.

Generalized travel time data misfit was used in this algorithm, which is the optimal time shift per well. Thus, reduce size of the matrix solution

c. Numerical stencil.

The numerical stencil technique based on efficient SVD (singular value decomposition) is used to calculate the square root of covariance matrix, which is fast and efficient and applicable to all kinds of covariance models.

d. Time Scaling Property.

The CPU time scales linearly compared with square scaling property in conventional approach.

(2) The high computational efficiency due to above advantages makes it particularly suitable for uncertainty assessment of large-scale field cases. We demonstrate the utility

of our approach along with Randomized Likelihood Maximum in uncertainty assessment using a field example.

(3) It is important to exhaust available quantified information in the priors before integration of dynamic data.

By the collocated sequential Gaussian simulation, the prior distribution of permeability field is better modeled than that from cloud transform. The explanation is that, in collocated SGS, the information of spatial relation among prior data is integrated by modeling of the covariance matrix of them while in the cloud transform, no information on spatial property of permeability and porosity and relation between them is included.

5.2 Recommendations

In our current approach, the 5x5x5 stencil was used to approximate the square root of the prior covariance matrix, which is a trade-off between the accuracy and the computational efficiency.

Streamline-based sensitivity has unique advantage in term of its fast sensitivity calculation. Generalization the sensitivity to full three phases will eventually make this method more applicable and precise.

The integration of static data such as the well logging and seismic is done by integrated the data derived from well logging (permeability) and seismic (porosity) respectively. The direct integration of seismic and well logging through one common proxy (such as elastic property of formation) might decrease the loss of data precision by decreasing the artificiality or by decreasing the steps of data explanation.

To generate multiple equally probable models honoring prior information, the sequential Gaussian simulation based on the variogram has been widely used. However, as statistical tool quantify the dissimilarity of variable at two spatial sites, variogram is not a necessary good measure of special heterogeneity in the geological sense. It is far from exhausting the prior geological information other than two point quantitative relations. Also, the hidden assumptions of stationarity, ergodicity and preferred

multivariate Gaussian distribution idealizes and oversimplifies the geological complexity and reality.

NOMENCLATURE

$\Delta \tilde{t}$	= Generalized travel time shift
Λ	= Diagonal matrix whose diagonal are the eigenvalues of the covariance matrix
λ_t	= Total mobility ratio
τ	= Time of flight
δm	= Change in the model parameter
Δt_j	= Time shift at well j
$\Delta x, \Delta y, \Delta z$	= Cartesian grid block sizes
a	= Range of reservoir parameter in the x-direction
b	= Range of reservoir parameter in the y-direction
C	= Range of reservoir parameter in the z-direction
C_d	= Data covariance matrix
C_M	= Prior covariance matrix of the model parameter
d	= Column vector with observed data
e	= Residual of the objective function $F(m)$
<i>Exp, Sph</i>	= Exponential and spherical covariance models, respectively
<i>Gauss</i>	= Gaussian covariance model
$F(m)$	= Objective function of Bayesian formulation
F_w	= Fractional flow of water
G	= Sensitivity matrix
$G(m)$	= Column vector with calculated reservoir performance data
H	= Hessian of the objective function $F(m)$
J	= Jacobian of the objective function $F(m)$. Gradient of e
J_p	= Misfit objective function
J^T	= Transpose of the jacobian
K	= Permeability
L	= Last time step (last data point)
M	= Number of model parameters
m	= Column vector of the reservoir parameter
m_p	= Column vector with prior knowledge of reservoir parameter
n_d	= Number of data points
N_{dj}	= Number of data points at well j
n_w	= Number of wells
N_x, N_y, N_z	= Number of grid blocks in the x, y, and z direction, respectively
P	= Pressure
R^2	= Coefficient of determination
s	= Slowness
S_w	= Water saturation
t	= Time
U	= Matrix whose column are the eigenvectors of the covariance
U^T	= Transpose of matrix X

W_{ij}	= Data weight for each data point (i) and at well (j)
y_j^{cal}	= Calculated data at well j
y_j^{obs}	= Observed data at well j
ϕ	= Porosity
σ^2	= Variance of reservoir parameter

REFERENCES

1. Gavalas, G.R., Shah, P.C. and Seinfeld, J.H.: "Reservoir History Matching by Bayesian Estimation," paper SPE 5740 presented at the 1976 SPE-AIME 4th Symposium on Numerical Simulation of Reservoir Performance, Los Angeles, CA, 19-20 Feb.
2. Reynolds, A.C., He, N., and Oliver, D.S.: "Reducing Uncertainty in Geostatistical Description with Well Testing Pressure Data," paper presented at the 1997 International Reservoir Characterization Conference, Houston, TX, 2-4 March.
3. Oliver, D.S.: "Incorporation of Transient Pressure Data into Reservoir Characterization," *In Situ* (1994) **18**, 13.
4. Li, R, Reynolds, A. C., and Oliver, D. S.: "History Matching of Three-Phase Flow Production Data," paper SPE 66351 presented at the 2001 Reservoir Simulation Symposium, Houston, TX, 11-14 Feb.
5. Wu, Z., Reynolds, A. C., and Oliver, D. S.: "Conditioning Geostatistical Models to Two-Phase Production Data," *SPEJ* (June 1999) 142.
6. Zhang, F., Skjervheim, J. A., Reynolds, A. C. and Oliver, D. S.: "Automatic History Matching in a Bayesian Framework, Example Applications," paper SPE 84461 presented at the 2003 SPE Annual Technical Conference and Exhibition, Denver, CO, 5-8 October.
7. Wu, Z. and Datta-Gupta, A.: "Rapid History Matching Using a Generalized Travel Time Inversion Method," *SPEJ* (June 2002) 113.
8. Vasco, D.W., Yoon, S., and Datta-Gupta, A.: "Integrating Dynamic Data into High-Resolution Reservoir Models Using Streamline-Based Analytic Sensitivity Coefficients," *SPEJ* (December 1999) 389.
9. He, Z., Datta-Gupta, A., and Yoon, S.: "Streamline-Based Production Data Integration with Gravity and Changing Field Conditions," *SPEJ* (December 2002) 423.

10. Cheng, H., Kharghoria, A., He, Z., and Datta-Gupta, A.: "Fast History Matching of Finite-Difference Models Using Streamline-Derived Sensitivities," paper SPE 89447 presented at the 2004 SPE/DOE 14th Symposium on Improved Oil Recovery, Tulsa, OK, 17-21 April.
11. Vasco, D.W., and Datta-Gupta, A.: "Integrating Multiphase Production History in Stochastic Reservoir Characterization," *SPEFE* (September 1997) 149.
12. Cobenas, R.H., Aprilian, S.S., and Datta-Gupta, A.: "A Closer Look at Non-Uniqueness During Dynamic Data Integration into Reservoir Characterization," paper SPE 39669 presented at the 1998 SPE/DOE Improved Oil Recovery Symposium, Tulsa, OK, 19-22 April.
13. Vega, L., Rojas, D., and Datta-Gupta, A., "Scalability of the Deterministic and Bayesian Approaches to Production Data Integration into Field-Scale Reservoir Models," paper SPE 79666 presented at the 2003 SPE Reservoir Simulation Symposium, Houston, TX, 3-5 February.
14. Liu, N., Betancourt, S., and Oliver, D.S.: "Assessment of Uncertainty Assessment Methods," paper SPE 71624 presented at the 2001 SPE Annual Technical Conference and Exhibition, New Orleans, 30 September- 3 October.
15. Ahmed, M.D.: *Automatic History Matching in Bayesian Framework for Field-scale Applications*, Ph.D. dissertation, Texas A&M University, College Station, (2004).
16. Chu, L., Reynolds, A.C., He, N., and Oliver, D.S.: "Computation of Sensitivity Coefficients for Conditioning the Permeability Field to Well-test Pressure Data," *In Situ* (1995) **19**, 86.
17. Nocedel, J. and Wright, S. J.: *Numerical Optimization*, Springer-Verlag, New York (1999).
18. Vega, L., *An Efficient Bayesian Formulation for Production Data Integration into Reservoir Models*, Ph.D. dissertation, Texas A&M University, College Station, (2003).

19. Anterion, F., Karcher, B., and Eymard, R.: "Use of Parameter Gradients for Reservoir History Matching," paper SPE 18433 presented at the 1989 SPE Reservoir Simulation Symposium, Houston, TX, 6-8 February.
20. Chen, W.H., Gavalas, G.R., Seinfeld, J.H., and Wasserman, M.L.: "A New Algorithm for Automatic History Matching," *SPEJ* (December 1974) 593.
21. Chavent, G. M., Dupuy, M., and Lemonnier, P.: "History Matching by Use of Optimal-Control Theory," *SPEJ* (February 1975) 74.
22. Wasserman, M.L., Emanuel, A.S., and Seinfeld, J.H.: "Practical Applications of Optimal Control Theory to History Matching Multiphase Simulator Models," *SPEJ* (August 1975) 347.
23. Watson, A.T., Seinfeld, J.H., Gavalas, G.R., and Woo, P.T.: "History Matching in Two-Phase Petroleum Reservoirs," *SPEJ* (December 1980) 521.
24. Tarantola, A.: *Inverse Problem Theory – Methods for Data Fitting and Model Parameters Estimation*, Elsevier, New York, (1987).
25. Oliver, D.S.: "Calculation of the Inverse of the Covariance," *Mathematical Geology* (1998) **30**, 911.
26. Cheng, H., Datta-Gupta, A., and He, Z.: "A Comparison of Travel Time and Amplitude Matching for Field-Scale Production Data Integration: Sensitivity, Non-Linearity and Practical Implications," paper SPE 84570 presented at the 2003 SPE Annual Technical Conference and Exhibition, Denver, CO, 5-8 October.
27. Oliver, D.S., He, N., and Reynolds, A.C.: "Conditioning Permeability Fields to Pressure Data," presented at the 1996 European Conference on the Mathematics of Oil Recovery, Leoben, Austria, 3-6 September.
28. Paige, C.C. and Saunders, M.A., "LSQR: An Algorithm for Sparse Linear Equations and Sparse Least Squares," *ACM Transactions on Mathematical Software* (March 1982) **8**, 43.
29. Nolet, G.: "Seismic Wave Propagation and Seismic Tomography," *Seismic Tomography*, (March 1987) 1.

30. Kitanidis, P.K.: “Quasi-linear Geostatistical Theory for Inversing,” *Water Resour. Res.* (1995) **31**, 2411.
31. Wilks, S.S.: *Mathematical Statistics*, John Wiley and Sons, New York (1962)
32. Aly, A., Lee, W.J., Datta-Gupta, A., Mowafi, K., Prida, M., and Latif, M.: “Application of Geostatistical Modeling in an Integrated Reservoir Simulation Study of the Lower Bahariya Reservoir, Egypt,” paper SPE 53118 presented at the 1999 Middle East Oil Show and Conference , Bahrain, 20-23 February.

VITA

Chengwu Yuan
 Petroleum Engineering Department.
 3116 TAMU
 College Station, TX USA, 77843
 Chengwu_yuan@yahoo.com

EDUCATION

- Master of Science** Petroleum Engineering. Texas A&M University
 December 2005
- Master of Science** Petroleum Engineering. University of Petroleum, Beijing
 February 1997
- Bachelor of Science** Production Engineering. China University of Petroleum
 July 1992

WORK EXPERIENCE

Schlumberger Consulting Services U.S. Land East, TX. (Summer Internship, 2005)

Data collection and processing

Texas A&M University, Research Assistance of Dr. Akhil Datta Gupta, (9/03 ~5/05)

Data Integration and automatic history matching

Stochastic modeling & uncertainty analysis

Streamline simulation

University of Petroleum (Beijing), China (1997~ 2003)

* Research focus:

Well Stimulation and Optimization by Numerical and Physical Simulation of Flow.

* Vice Lecturer for “Flow Dynamics in Porous Media ” (1999~2003)

Shingle Oil Field, Shandong, China (1992~ 1993) **Field Engineer**

Hands-on experience in well stimulation and down hole operations.